Radiotherapy and Oncology 95 (2010) 60–65

Contents lists available at ScienceDirect

Radiotherapy and Oncology

journal homepage: www.thegreenjournal.com

Carbon ion radiation therapy

Dose–volume histogram and dose–surface histogram analysis for skin reactions to carbon ion radiotherapy for bone and soft tissue sarcoma

Takeshi Yanagi *, Tadashi Kamada, Hiroshi Tsuji, Reiko Imai, Itsuko Serizawa, Hirohiko Tsujii

Research Center Hospital for Charged Particle Therapy, National Institute of Radiological Sciences, Chiba, Japan

ARTICLE INFO

Article history:
Received 17 March 2009
Received in revised form 24 August 2009
Accepted 27 August 2009
Available online 18 September 2009

Keywords:
Dose–volume histogram
Dose–surface histogram
Carbon ion radiotherapy
Bone and soft tissue sarcoma
Skin reaction
Skin ulcer

ABSTRACT

Background and purpose: To evaluate the usefulness of the dose–volume histogram (DVH) and dose–surface histogram (DSH) as clinically relevant and available parameters that helped to identify bone and soft tissue sarcoma patients at risk of developing late skin reactions, including ulceration, when treated with carbon ion radiotherapy.

Materials and methods: Thirty-five patients with bone and soft tissue sarcoma treated with carbon ion beams were studied. The clinical skin reactions were evaluated. Some pretreatment variables were compared with the grade of late skin reactions.

Results: Average DVH and DSH were established in accordance with the grading of the skin reactions. Prescribed dose, the difference in depths between the skin surface and the proximal extent of the tumor, and some DVH/DSH parameters were correlated with late skin reaction (≥grade 3) according to univariate analysis. Furthermore, the area irradiated with over 60 GyE (S_{60} > 20 cm^2) on DSH was the most important factor by multivariate analysis.

Conclusions: The area irradiated with over 60 GyE (S_{60} > 20 cm^2) on DSH was found to be a parameter for use as a predictor of late skin reactions.

 Radiotherapy and Oncology 95 (2010) 60–65

In 1994, clinical research trials using carbon ion beams were initiated at the National Institute of Radiological Sciences (NIRS) in Chiba, Japan [1–3]. As of February 2008, a total of 3819 patients (4053 lesions) have been treated by this modality. Some of these patients, especially those with bone and soft tissue sarcoma, had tumors located near the skin and developed severe skin reactions after treatment [3]. Among them, some progressed to grade 4 late skin reactions identified as ulcers. To allow the prediction of such skin reactions, it is useful to search for factors that are related to the skin reactions. Thus, in this study, certain factors of patients with bone and soft tissue sarcoma were assessed in terms of correlation with late skin reactions associated with the clinical use of carbon ion radiotherapy.

Materials and methods

Protocol study

From June 1996 to December 1999, 64 lesions in 57 patients (37 men and 20 women) with unresectable bone and soft tissue sarcoma were treated with carbon ion beams according to our dose escalation protocol. The patient eligibility of this protocol was described previously [3]. Briefly, they had histologically confirmed bone and soft tissue sarcomas judged unresectable by the referring surgeon. The tumor had to be grossly measurable, but its size was not allowed to exceed 15 cm. For dose escalation, at least 3 patients each were treated at the same dose level, and then, after careful observation, a 10% total-dose escalation was conducted. All patients signed informed consent forms approved by the local institutional review board.

Patient selection criteria

For the sake of accuracy and simplicity of evaluation, the following patients were excluded from the analysis: (1) those with tumor invasion into the skin, which might complicate the direct radiation effect on the skin; (2) those who died within six months (in the case of acute skin evaluation) or within 1.5 years (in the case of late skin evaluation) after treatment; (3) those treated in both supine and prone positions because they required recalculation of the total dose of both positions using a pseudo-target; and (4) those with tumors located in a limb, because skin reactions of limbs show different patterns from those of other sites, and should be dealt with separately. After these adjustments, 35 patients (35 lesions) were analyzed for acute skin reactions and 27 of these patients (27 lesions) were also analyzed for late skin reactions.

* Corresponding author. Address: Research Center Hospital for Charged Particle Therapy, National Institute of Radiological Sciences, Anagawa 4-9-1, Inage Ward, Chiba City, Chiba Prefecture 263-8555, Japan.
E-mail address: tyana@med.nagoya-cu.ac.jp (T. Yanagi).

0167-8140/$ - see front matter
doi:10.1016/j.radonc.2009.08.041

Carbon ion radiotherapy

Carbon ion beams were generated by HIMAC (Heavy Ion Medical Accelerator in Chiba), the world's first heavy ion accelerator complex dedicated to medical use in a hospital environment [1]. The energy levels of the generated beams were 290 MeV, 350 MeV, and 400 MeV. For the treatment, the patients were positioned in customized cradles (Moldcare; Alcare, Tokyo, Japan) and were immobilized with a low-temperature thermoplastic retaining device. A set of 5-mm-thick slice CT images was taken for treatment planning with the patients retained in the immobilization device. Three-dimensional treatment planning was performed using HIPLAN software (by NIRS) [4].

In accordance with the ICRU Report [5], the visible lesion on the CT image was defined as the gross tumor volume (GTV). The clinical target volume (CTV) included the GTV and the estimated subclinical local involvement. An internal margin was added to the CTV to allow for tumor movement and tumor growth. The planning target volume (PTV) consisted of the CTV, the internal margin, and a set-up margin corresponding to the sum of the error lengths at positioning (about half the length of the CT slice thickness in our system) including the dose calculation error associated with the change from the CT value to the beam range (about 3% at our system). As a result, a margin of about 5 mm was usually added to the CTV to create the PTV. The PTV was covered by at least 90% of the administered dose.

Dose was expressed in Gray equivalent (GyE), which was calculated by multiplying the physical dose with the Relative Biological Effectiveness (RBE). The RBE was estimated to be 3.0 at the distal part of the spread-out Bragg peak (SOBP) based upon radiobiological studies. The details of the RBE value used at NIRS were discussed by Kanai et al. [6].

Skin evaluation

Four radiation oncologists score-rated all the skin reactions of each patient in the maximum phase by checking the photo-slides captured during the follow-up durations, using the RTOG Scoring System for assessing acute reactions and the Late Radiation Morbidity Scoring Scheme of RTOG/EORTC for evaluating the late skin reactions [7].

Dose–volume histogram (DVH) and dose–surface histogram (DSH)

DVH was calculated for the region of interest (ROI). ROI was defined as all the organs inside the body covered by the skin at the irradiated area. DSH was calculated by the following procedure. First, the skin contours were carefully outlined with a thickness of one pixel for each CT slice. Then, the contours of the skin surface on each CT slice were divided into small (5 mm) compartments, and multiplied by the thickness of the CT slice (5 mm). In this manner, a number of 25-mm^2 square-shaped compartments with one-pixel-sized-thickness volume were made. The next step was to calculate the radiation dose delivered to each of these compartments. The equal-dose compartments were then summated to determine the cumulative area irradiated with each discrete dose level so as to obtain the cumulative DSH. The calculation of DVH and DSH was performed using HIPLAN software [4].

Evaluation of pretreatment variables

Some of the pretreatment variables thought to be relevant to late skin reactions were assessed using Fisher's exact test in univariate analysis. The variables contained sex, patient age, primary tumor site, difference in depths between the skin surface and the proximal extent of the tumor, planning target volume, prescribed dose, neoadjuvant chemotherapy, and adjuvant chemotherapy. Furthermore, some factors with significance in univariate analysis and the representative values derived from DVH/DSH parameters were applied to multivariate analysis using Cox's proportional hazard model.

Results

Patient and tumor characteristics

All 35 patients with acute skin reactions and 27 patients with late skin reactions were analyzed. The number of lesions and patients was the same. Table 1 shows the patients' and tumor characteristics. The numbers of patients at each total-dose level were 3 (52.8 GyE), 6 (57.6 GyE), 6 (64 GyE), 5 (70.4 GyE), and 15 (73.6 GyE) for acute skin reactions, and 3 (52.8 GyE), 3 (57.6 GyE), 5 (64 GyE), 4 (70.4 GyE), and 12 (73.6 GyE) for late skin reactions. All the patients were treated in fixed 16 fractions. In the patients analyzed for late skin reactions, more than one-third of the tumors were located in the sacral region.

Follow-up and skin reactions

After the treatment, the patients were examined on a regular basis throughout the follow-up period. Maximum follow-up time in these patients ranged from 29.5 to 71.7 months (median 44.7 months).

Table 1
Patients' and tumor characteristics.

	Acute evaluation	Late evaluation
Numbers	35	27
Age/median (years)	15–85/47	15–85/51
Gender		
Male	22 (62.9%)	18 (66.7%)
Female	13 (37.1%)	9 (33.3%)
Tumor site		
Sacrum	11 (31.4%)	10 (37.0%)
Spine	10 (28.6%)	8 (29.6%)
Iliac bone	6 (17.1%)	3 (11.1%)
Pubic bone	4 (11.4%)	3 (11.1%)
Others	4 (11.4%)	4 (11.1%)
Target volume/median (ml)	49–1829/714	49–1665/701
Target dose		
52.8 GyE	3 (8.6%)	3 (11.1%)
57.6 GyE	6 (17.1%)	3 (11.1%)
64.0 GyE	6 (17.1%)	5 (18.5%)
70.4 GyE	5 (14.3%)	4 (14.8%)
73.6 GyE	15 (42.9%)	12 (44.4%)
Histologic diagnosis		
Bone		
Osteosarcoma	9 (25.7%)	8 (30.0%)
Chordoma	9 (25.7%)	9 (33.3%)
Chondrosarcoma	3 (18.6%)	2 (7.4%)
Others	3 (18.6%)	0 (0%)
Soft tissue		
MPNST[a]	4 (11.4%)	2 (7.4%)
MFH[b]	1 (2.9%)	0 (0%)
Liposarcoma	1 (2.9%)	1 (3.7%)
Others	5 (14.3%)	5 (18.5%)
Chemotherapy		
Neoadjuvant (+)	19 (54.3%)	14 (51.9%)
Neoadjuvant (−)	16 (45.7%)	13 (48.1%)
Adjuvant (+)	8 (22.9%)	6 (22.2%)
Adjuvant (−)	27 (77.1%)	21 (77.8%)

[a] Malignant peripheral nerve sheath tumor.
[b] Malignant fibrous histocytoma.

The outcome of the skin reactions is presented in Tables 2 and 3. Four patients developed late grade 4 skin reactions (ulceration). Patients who developed grade 3 or 4 late skin reactions had been prescribed with 70.4 GyE or more to the PTV. Three out of 4 patients who indicated grade 4 late skin reactions had the tumor located in the sacrum. The site of the skin reactions of these patients was at the gluteal fold.

The time of onset of late grade 3 varied from 6 months to 29 months, and that of late grade 4 varied from 8 months to 21 months after the initiation of the irradiation. The patients developing ulceration corresponding to a late grade 4 skin reaction needed surgery for recovery.

Dose–volume histogram and dose–surface histogram

In the dose–volume histograms and dose–surface histograms, the patients who received relatively high doses to their volumes or areas developed grade 3 or 4 reactions. DSH for all the patients graded by acute skin reaction is shown in Fig. 1. In order to understand their general trend, the average DVHs for some grade groups – grade 0 + 1, grade 2, grade 3, and grade 4 – for acute and late skin reactions are presented (figure for late skin reaction is shown in Fig. 2). There was a tendency for the curves to be separated from each other on the high dose side, which was above 56 GyE with regard to acute reactions (figure is not shown) and above 52 GyE with respect to late reactions. Concerning DSH, when we divided the patients into three groups, namely grade 0 + 1, grade 2, and grade 3 + 4, the average area for patients with acute and late grades 3 + 4 reactions was above the corresponding values for patients with grades 0 + 1 and/or grade 2 in almost all the graphs (figure for late reaction is shown in Fig. 3).

To find the representative parameters of the DVH values to use for the prediction of the late skin reaction, at first, the correlation between cumulative irradiated volume value sets at every dose in 2-GyE increments from 2 GyE to 74 GyE (V_2–V_{74}) of DVH and the grades of the late skin reactions (≥grade 3 vs. <grade 3) were evaluated by a nonparametric test, the Spearman's correlation test. The results showed that the values of V_{64} and V_{68} were correlated with the late skin reactions and became candidates for prognostic parameters. In the same manner, the values between S_{56} and S_{64} were derived from DSH as candidates. Then, we set the "cut-off volume" or "cut-off surface area" for each representative value at 100 ml or 10 cm^2 increments, which divided the lesions (patients) into two groups – above and below the cut-off levels. Then, the DVH or DSH parameters grouped by each cut-off level and late clinical reaction were evaluated. Finally, the $V_{64} > 100$ ml for DVH, and $S_{60} > 20$ cm^2 for DSH were selected as the candidates for predicting late skin reactions.

As for the consequential correlation between DVH/DSH and skin reaction achieved, the probability of grade 3 late skin reaction in patients with $V_{64} > 100$ ml and $V_{64} \leqslant 100$ ml was 60% and 8.3%, respectively, while that in patients with $S_{60} > 20$ cm^2 and $S_{60} \leqslant 20$ cm^2 was 100% and 22.7%, respectively.

Prognostic factors

On univariate analysis, the prescribed dose and the difference in depths between the skin surface and the proximal extent of the tumor were correlated with the development of late skin reactions (Table 4). On multivariate analysis among the difference in depths between the skin and the tumor, and the DVH/DSH parameters, the DSH parameter $S_{60} > 20$ cm^2 showed statistical significance ($p = 0.041$) (Table 5).

Correlation of acute skin and late skin reactions

In terms of the correlation between the grades of acute and late skin reactions, it was found that all lesions showed the same grade or a 1-grade difference between early and late reactions except for one lesion with a 2-grade difference (Fig. 4). Furthermore, among the four patients who developed late skin ulcerations, one patient failed to heal the acute moist desquamation and directly progressed into a late phase of the skin reaction.

Table 2
Outcome of skin reactions (1).

Dose (GyE)	Acute skin reaction						Late skin reaction					
	Grade of RTOG					Total	Grade of RTOG/EORTC					Total
	0	1	2	3	4		0	1	2	3	4	
52.8	0	2	1	0	0	3	0	2	1	0	0	3
57.6	0	2	4	0	0	6	0	3	0	0	0	3
64.0	1	4	1	0	0	6	1	3	1	0	0	5
70.4	0	1	2	2	0	5	0	1	0	2	1	4
73.6	0	2	7	5	1	15	0	3	2	4	3	12
Total	1	11	15	7	1	35	1	12	4	6	4	27

Table 3
Outcome of skin reactions (2).

Site	Acute skin reaction						Late skin reaction					
	Grade of RTOG					Total	Grade of RTOG/EORTC					Total
	0	1	2	3	4		0	1	2	3	4	
Sacrum	0	1	4	6	0	11	0	1	3	3	3	10
Spine	1	4	4	1	0	10	1	4	1	2	0	8
Iliac bone	0	1	4	0	1	6	0	1	0	1	1	3
Pubic bone	0	2	2	0	0	4	0	3	0	0	0	3
Others	0	3	1	0	0	4	0	3	0	0	0	3
Total	1	11	15	7	1	35	1	12	4	6	4	27

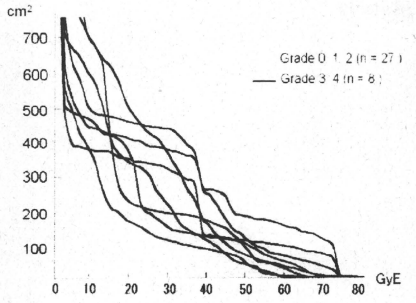

Fig. 1. DSH for all the patients grading by acute skin reaction (grade 0 + 1 + 2 vs. grade 3 + 4). In the dose–surface histograms, the patients who received relatively high doses to their surface area indicated grade 3 or 4 reactions.

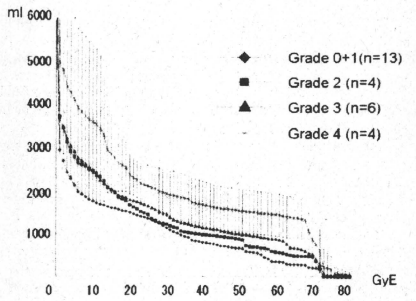

Fig. 2. Average DVH grading by late skin reactions (with the standard error bar of grade 4 reactions). There is a tendency for the curves to be separated from each other in the higher-dose part between 52 GyE and 74 GyE with respect to late reactions ($n = 27$).

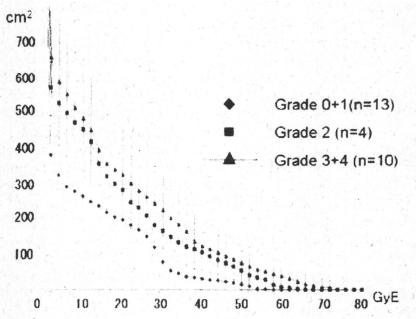

Fig. 3. Average DSH grading by late skin reactions (with the standard error bar of grade 3 + 4 reactions). The curves were also separated from each other throughout the whole dose part of the graph ($n = 27$).

Table 4
Univariate analysis (late reactions ⩾ grade 3).

		Odds ratio (95% CI)
Sex	(M, F)	1.27 (0.23–6.82)
Age	(⩾55 year,<55 year)	2.4 (0.47–12.13)
Primary tumor site	(Sacrum, other)	4.87 (0.89–26.42)
Planning target volume	(⩾900 ml,<900 ml)	3.11 (0.52–18.38)
Prescribed dose	(⩾70.4 GyE,<70.4 GyE)	–
Neoadjuvant chemotherapy	(+, –)	0.88 (0.18–4.24)
Adjuvant chemotherapy	(+, –)	5 (0.71–34.91)
Difference in depths[a]	(<2 cm,⩾2 cm)	10.12 (1.04–98.49)

[a] Difference in depths between skin and tumor.
* p Value < 0.05.

Table 5
Multivariate analysis (late reactions ⩾ grade 3).

	p Value	Hazard ratio	CI (95%)
Difference in depth between skin and tumor	0.657	1.669	0.174–15.998
Dose–volume histogram (V_{64} > 100 ml)	0.189	4.743	0.466–48.284
Dose–surface histogram (S_{60} > 20 cm²)	0.041*	5.107	1.068–24.420

Cox hazard model.
* p Value < 0.05.

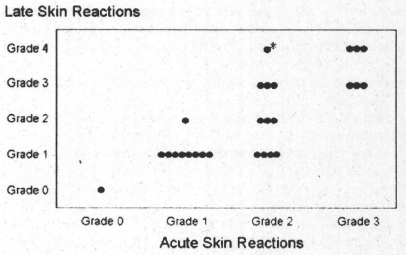

Fig. 4. Correlation between the grades of acute and late skin reactions. All patients showed the same grade or a 1-grade difference between early and late reactions except for one patient (*) with a 2-grade difference.

Discussion

In this study, acute and late skin reactions of the patients with bone and soft tissue sarcoma treated with carbon ion beams were evaluated, and a parameter for use as a predictor of late skin reactions was proposed.

In general, skin reactions to radiotherapy are divided into acute phase and late phase reactions. In acute radiation dermatitis the parenchyma of the skin, i.e., the epidermis, plays a leading role, and in the chronic phase it is the dermis and the subcutis that dominate the radiation injury to the skin. In terms of the degree of the normal tissue reaction, it is known that this is connected with the volume effect. Animal experiments have shown that the size of the irradiated field is associated with the intensity of the skin reactions [8]. Furthermore, the highly significant increase in incidence and severity was reported with increasing field size in the human skin. [9]. Therefore, it may be possible to predict skin reactions if we apply the dose–volume histogram or dose–surface histogram relating to the epidermis, dermis, and the subcutaneous tissues also to the human skin.

What kind of dose-related histogram is suitable for the evaluation of such skin reactions? We tried using two types of histograms in an attempt to answer this question. Firstly, we used the DVH whose ROI was defined as all the organs inside the body covered by the skin at the irradiated area. The reasons for choosing this type of DVH were its ease of preparation with any planning system and the advantages of having a simpler DVH for routine clinical practice. Since this DVH contains the entire volume within the contour, however, the histogram may be influenced by the size of the PTV.

Secondly, we calculated the DSH derived from the skin surface. This calculation was performed based on the hypothesis that the skin surface had the volume of one-pixel-sized-thickness (one pixel: i.e., 0.78–1.26 mm length). According to some reports, attempts for hollow organs have also had satisfactory success with assessing the histogram based on only the outer contour of the organ [10,11]. Since the thickness of the epidermis is 0.15–1.5 mm, this ROI will mainly represent the epidermis.

Other studies have reported the merits of using a band-like region as the ROI, such as a dose–wall histogram, when evaluating the dose of a hollow organ such as the rectum in treating prostate cancer [12]. Since irradiation of subcutaneous tissue affects clinical skin reactions, it may be preferable to use a dose–wall histogram whose ROI includes both the skin and subcutaneous tissue to evaluate the skin reaction. However, as it is not clear over what width range the subcutaneous tissue should be correlated with the development of the skin reaction, it is difficult to adopt an adequate wall width when using a dose–wall histogram. Furthermore, the tumor volume included in the ROI depends largely on how to define the width of the wall. Therefore, a dose–wall histogram is not necessarily adequate for skin evaluation. According to our results, both histograms (DVH/DSH) were correlated with the clinical skin reactions in a certain part of the graph, substantiating the validity of our approach.

There are many reports that discuss skin reactions after X-ray radiotherapy [13,14]. Emami et al. reported a probability of 5% skin necrosis within five years from treatment with 60 Gy for a 30-cm^2 field and 70 Gy for a 10-cm^2 field [13]. Giro et al. reported that high rate of severe radiation dermatitis was observed during radiation therapy with concurrent systemic drug: cetuximab, and they recommended interrupting further treatment if confluent moist desquamation occurs at total doses below 40 Gy [14]. However, carbon ion beams lack the build-up phenomenon, so that the data from X-ray cannot be applied directly to patients treated with carbon ion beams.

Although carbon ion radiotherapy is still in the pioneering stage, many patients have already been treated with fast neutrons, another of the high LET radiation treatment modalities. After treatment with fast neutrons, late damage was greater than that expected on the basis of the early reactions that had been observed [15,16]. This was partly because the relative biological effectiveness (RBE) for late reactions was in general greater than that for acute reactions [17].

The RBE value of carbon ions produced for the therapy at the Institute at Chiba was initially estimated as 3.0 at the distal part of the SOBP (around 8 mm upstream from the distal peak of the SOBP) [6], and we changed the RBE value according to the average LET in the SOBP based on the biological experiments (Fig. 5). Although it was initially well recognized that RBE values changed with fractionation schedule, total dose, and the effect accessed, at the start of the clinical trials in the Institute the RBE was kept constant, even when the fractionation schedule was changed to avoid confusion in clinical trails [6].

In this paper, the institutional protocol was still adopted (GyE = physical dose × RBE), because the study was deeply correlated with practical clinical use. In the future, further clinical observations of the normal tissue reaction after carbon ion radiotherapy might lead to more suitable RBE values for various normal tissues and various fractionation schedules.

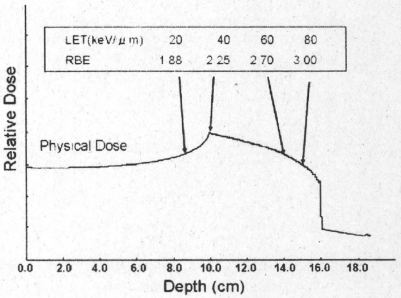

Fig. 5. RBE and LET values used in clinical study (carbon ion, 290 MeV, SOBP = 60 mm). Average LET at the depth was used. The relationship between RBE and LET was obtained from the biological experiments preceded to the commencement of clinical studies [6].

From the results of the present study, all the lesions developing grade 3 or 4 late skin reactions were treated with more than 70.4 GyE as the prescribed dose to the PTV (Table 2). Univariate analysis showed the correlation between the prescribed dose and the late skin reaction (Table 4). It was indicated that severe skin reaction may not develop if the prescribed dose is 64 GyE or less. However, the local control rate of bone and soft tissue sarcomas is dose-dependent. According to Kamada et al., the local control rates of patients receiving 64 GyE or more were significantly better than those of patients with 52.8–57.6 GyE [3], meaning that a higher dose should be used for good local control. Thus, some reliable prognostic parameters are called for.

As shown in Table 3, 3 of the 4 patients who developed grade 4 late skin reactions had the tumor located in the sacrum. The sites of the skin reactions of these patients were at the gluteal fold. This region is notorious for developing decubitus ulcer easily. However, almost all the patients who were treated in the sacral region in this study spent their time in a prone position because of their pain. Thus, these ulcers may be correlated with the irradiation mainly, not mechanical pressure.

It has also been found that the DSH parameter ($S_{60} > 20$ cm^2) was better suited than the DVH parameter ($V_{64} > 100$ ml) for evaluating late skin reactions. This may suggest that skin reactions, even in the late phase, are mainly related to superficial parts of the skin. Recent reports using intensity-modulated radiation therapy (IMRT) suggest that for the sake of avoiding severe skin reactions it might be more effective to plan the PTV a little removed from the skin [18]. In NIRS, we have already obtained successful results with similar methods applied for carbon ion irradiation. Thus, from a clinical point of view, the importance of the superficial parts of the skin in late skin reactions is clearly indicated.

Although no direct relationship was found to exist between the acute and late reactions, the present study showed that a tendency of a relationship does exist between these two reactions for the specific dose fractionation schedule used for this group of patients. With the recent change from conventional radiotherapy to more aggressive schedules, it has been noted that a non-healing-related acute response can directly progress into a late effect. This late effect has been termed "consequential late effect" (CLE) [19]. CLEs are mainly found in those organ systems in which a barrier against mechanical or chemical stress is established by the acutely responding component, such as the urinary and intestinal systems, in mucosa and skin. Bentzen and Overgaard reported, for example,

based on the data of 229 patients, that patients who developed moist desquamation in the early reaction had a statistically significantly increased risk of developing telangiectasia in the late reaction after X-ray radiotherapy [20]. The observation, at the present study, that most lesions showed the same grade or a 1-grade difference between early and late reactions seemed to support these results. Furthermore, one patient developed consequential ulcer as a consequence of the development of early moist desquamation that is difficult to heal. This case was considered CLE.

Conclusion

Skin was a critical organ in heavy charged particle radiotherapy, with multiple factors contributing to skin reactions. The area irradiated with over 60 GyE (S_{60} > 20 cm^2) on DSH was found to correlate significantly with late skin reactions (≧grade 3).

Acknowledgements

The authors thank Mitsuji Wakaisami, Hiroshi Asakura and Norikazu Tanabe, technologists, for their contribution of the DVH/DSH calculation.

References

[1] Tsujii H, Morita S, Miyamoto T, et al. Preliminary results of phase I/II carbon ion therapy at National Institute of Radiological Sciences. J Brachyther Int 1997;13:1–8.
[2] Tsujii H, Morita S, Miyamoto T, et al. The current status and perspective of heavy-ion therapy. In: Proceedings of the sixth international meeting on progress in radio-oncology, Bologna, Monduzzi Editore S.p.A; 1998. p. 709–21.
[3] Kamada T, Tsujii H, Tsuji H, et al. Efficacy and safety of carbon ion radiotherapy in bone and soft tissue sarcoma. J Clin Oncol 2002;20:4466–71.
[4] Endo M, Koyama-Ito H, Tsujii H, et al. HIPLAN – a heavy ion treatment planning system at HIMAC. J Jpn Soc Ther Radiol Oncol 1996;8:231–8.
[5] International commission on radiation units and measurements. Prescribing, recording, and reporting photon beam therapy (supplement to ICRU Report 50). ICRU Report 62, Bethesda; 1999. p. 3–20.
[6] Kanai T, Endo M, Minohara S, et al. Biophysical characteristics of HIMAC clinical irradiation system for heavy-ion radiation therapy. Int J Radiat Oncol Biol Phys 1999;44:201–10.
[7] Cox JD, Stetz BS, Pajak TF. Toxicity criteria of the Radiation Therapy Oncology Group (RTOG) and the European Organization for Research and Treatment of Cancer (EORTC). Int J Radiat Oncol Biol Phys 1995;31:1341–6.
[8] Hopewell JW. Mechanisms of the action of radiation on skin and underlying tissues. Br J Radiol (Suppl) 1986;19:39–51.
[9] Bentzen SM, Saunders MI, Dische S, et al. Radiotherapy-related early morbidity in head and neck cancer: quantitative clinical radiobiology as deduced from the CHART trial. Radiother Oncol 2001;60:123–35.
[10] Fenwick JD, Khoo VS, Nahum AE, et al. Correlations between dose–surface histograms and the incidence of long-term rectal bleeding following conformal or conventional radiotherapy treatment of prostate cancer. Int J Radiat Oncol Biol Phys 2001;49:473–80.
[11] Meijer GJ, van den Brink M, Hoogeman MS, et al. Dose–wall histograms and normalized dose–surface histograms for the rectum: a new method to analyze the dose distribution over the rectum in conformal radiotherapy. Int J Radiat Oncol Biol Phys 1999;45:1073–80.
[12] Boersma LJ, van den Brink M, Bruce AM, et al. Estimation of the incidence of late bladder and rectum complications after high-dose (70–78 Gy) conformal radiotherapy for prostate cancer using dose–volume histograms. Int J Radiat Oncol Biol Phys 1998;41:83–92.
[13] Emami B, Lyman J, Brown A, et al. Tolerance of normal tissue to therapeutic irradiation. Int J Radiat Oncol Biol Phys 1991;21:109–22.
[14] Giro C, Berger B, Boelke E, et al. High rate of severe radiation dermatitis during radiation therapy with concurrent cetuximab in head and neck cancer: results of a survey in EORTC institute. Radiother Oncol 2009;90:166–71.
[15] Stone RS, Larkin JC. Treatment of cancer with fast neutrons. Radiology 1942;39:608–20.
[16] Duncan W. An evaluation of the results of neutron therapy trials. Acta Oncol 1994;33:299–306.
[17] Hall EJ. Radiobiology for the radiologist. 4th ed. Philadelphia: J.B. Lippincott; 1994. p. 157 and 217.
[18] Lee N, Chuang C, Quivey JM, et al. Skin toxicity due to intensity-modulated radiotherapy for head-and-neck carcinoma. Int J Radiat Oncol Biol Phys 2002;53:630–7.
[19] Doerr W, Hendry JH. Consequential late effects in normal tissues. Radiother Oncol 2001;61:223–31.
[20] Bentzen SM, Overgaard M. Relationship between early and late normal-tissue injury after postmastectomy radiotherapy. Radiother Oncol 1991;20:159–65.

Radiotherapy and Oncology 96 (2010) 231–235

Contents lists available at ScienceDirect

Radiotherapy and Oncology

journal homepage: www.thegreenjournal.com

Particle beam radiotherapy

Comparison of efficacy and toxicity of short-course carbon ion radiotherapy for hepatocellular carcinoma depending on their proximity to the porta hepatis

Hiroshi Imada [a,b,*], Hirotoshi Kato [a], Shigeo Yasuda [a], Shigeru Yamada [a], Takeshi Yanagi [a], Riwa Kishimoto [a], Susumu Kandatsu [a], Jun-etsu Mizoe [a], Tadashi Kamada [a], Osamu Yokosuka [b], Hirohiko Tsujii [a]

[a] National Institute of Radiological Sciences, Chiba, Japan; [b] Department of Medicine and Clinical Oncology, Chiba University, Japan

ARTICLE INFO

Article history:
Received 27 April 2009
Received in revised form 4 March 2010
Accepted 21 May 2010
Available online 25 June 2010

Keywords:
Radiotherapy
Carbon ion
Hepatocellular carcinoma
Porta hepatis

ABSTRACT

Background and purpose: To compare the efficacy and toxicity of short-course carbon ion radiotherapy (C-ion RT) for patients with hepatocellular carcinoma (HCC) in terms of tumor location: adjacent to the porta hepatis or not.

Materials and methods: The study consisted of 64 patients undergoing C-ion RT of 52.8 GyE in four fractions between April 2000 and March 2003. Of these patients, 18 had HCC located within 2 cm of the main portal vein (porta hepatis group) and 46 patients had HCC far from the porta hepatis (non-porta hepatis group). We compared local control, survival, and adverse events between the two groups.

Results: The 5-year overall survival and local control rates were 22.2% and 87.8% in the porta hepatis group and 34.8% and 95.7% in the non-porta hepatis group, respectively. There were no significant differences ($P = 0.252$, $P = 0.306$, respectively). Further, there were no significant differences in toxicities. Biliary stricture associated with C-ion RT did not occur.

Conclusions: Excellent local control was obtained independent of tumor location. The short-course C-ion RT of 52.8 GyE in four fractions appears to be an effective and safe treatment modality in the porta hepatis group just as in the non-porta hepatis group.

 Radiotherapy and Oncology 96 (2010) 231–235

Hepatocellular carcinoma (HCC) is one of the most common malignant tumors worldwide and is the third leading cause of death from cancer [1]. Various therapeutic options are presently available for patients with HCC. In radiotherapy, the role for patients with HCC was previously limited and unsatisfactory on the basis of its poor hepatic tolerance to irradiation [2,3]. Technological advances have made it possible to deliver a higher dose of radiation to focal liver tumors accurately, reducing the degree of toxicity [4–7]. Proton beam therapy was shown to be effective and safe for HCC, mainly due to its excellent dose distribution at the end of the beam path, called the Bragg peak [8–10]. Carbon ion beams also possess the Bragg peak, and they provide excellent dose distribution to the target volume by specified beam modulations [11–15]. They have advantageous biological and physical properties that result in a higher cytocidal effect than that of photons and protons [16–19]. Since 1995, carbon ion radiotherapy (C-ion RT) has been performed for treatment of HCC, and clinical trials were initiated at the National Institute of Radiological Sciences (NIRS).

In terms of HCC adjacent to the porta hepatis, treatment with minimal invasiveness and complications is an important issue. Surgical resection is the standard of curative treatment, but it is restricted to selected patients due to degradation of hepatic function [20,21]. Liver transplantation is a curative treatment of HCC, but it is often not feasible [22–24] and a shortage of donors also limits its possibilities. Radiofrequency ablation (RFA) and other ablative techniques obtain excellent local control, but are limited largely to small HCCs [25–27]. In the presence of blood vessels contiguous with tumor, blood flow reduces the thermal effects of RFA [28–30]. In addition, biliary complications after RFA for HCC adjacent to the porta hepatis sometimes occur, resulting in septic complications and liver failure [31].

We have already reported that C-ion RT used for the treatment of HCC is safe and effective [17,19]. In this study, patients were stratified into two groups according to tumor localization: adjacent to the porta hepatis or not. We compared the treatment effect and toxicity between the two groups retrospectively.

Materials and methods

Patients

Between April 2000 and March 2003, 64 patients with HCC underwent 52.8 GyE/4-fraction C-ion RT in a phase I/II clinical trial or phase II clinical trial at NIRS. The phase I/II clinical trial was carried out from April 2000 to March 2001, and the phase II clinical

* Corresponding author. Address: Research Center for Charged Particle Therapy, National Institute of Radiological Sciences, 4-9-1, Anagawa, Inage-ku, Chiba 263-8555, Japan.
E-mail address: h_imada@nirs.go.jp (H. Imada).

0167-8140/$ - see front matter © 2010 Elsevier Ireland Ltd. All rights reserved.
doi:10.1016/j.radonc.2010.05.019

Table 1
Patient and tumor characteristics.

	Total	Porta hepatis group	Non-porta hepatis group	P
N	64	18	46	
Gender, *n* (%)				>0.999
Male	48 (75)	14 (78)	34 (74)	
Female	16 (25)	4 (22)	12 (26)	
Age (years)				0.736
Median	69	68	69	
Range	37–84	51–79	37–84	
Child-Pugh classification, *n* (%)				0.198
A	49 (77)	16 (89)	33 (72)	
B	15 (23)	2 (11)	13 (28)	
Stage (UICC 5th), *n* (%)				0.438
II	23 (36)	5 (28)	18 (39)	
IIIA	32 (50)	9 (50)	23 (50)	
IVA	9 (14)	4 (22)	5 (11)	
Maximum tumor diameter (mm)				0.725
Median	40.0	36.5	40.0	
Range	12–120	21–120	12–112	
Vascular invasion				0.066
Yes	45 (70)	16 (89)	29 (63)	
No	19 (30)	2 (11)	17 (37)	
Number of tumors, *n* (%)				0.676
Single	56 (88)	15 (83)	41 (89)	
Multiple	8 (12)	3 (17)	5 (11)	

Abbreviations: UICC = International Union against cancer.

trial was sequentially performed from April 2001 to March 2003. The eligibility criteria were previously reported [17]. HCC was diagnosed by needle biopsy in all patients. Prior to treatment, all patients gave their informed consent in writing in accordance with the Declaration of Helsinki. These clinical trials were approved by the ethics committees at NIRS. Eighteen of the 64 patients had HCC located within 2 cm from the main portal vein, and the other 46 had HCC far from the porta hepatis.

Background data of the patients and tumors are presented in Table 1. The enrolled patients consisted of 48 males and 16 females. Median age was 69 years (range, 37–84). Child-Pugh classification of the degree of liver impairment was as follows: 49 patients were categorized as Class A (scores, 5–6), and 15 patients as Class B (scores, 7–9). Twenty-three patients had Stage II, 32 had Stage IIIA, and 9 had Stage IVA. By the Barcelona Clinic Liver Cancer staging classification [32,33], 2 patients had Stage A and 16 had Stage C in the porta hepatis group, and 15 had Stage A, 2 had Stage B, and 29 had Stage C in the non-porta hepatis group. Median maximum tumor diameter was 40 mm (range, 12–120). Forty-five patients had vascular invasion. Fifty-six patients had a solitary mass and 8 had multiple tumors.

Pretreatment evaluation

Laboratory values collected for all patients included complete blood cell counts, liver and renal function tests, electrolytes, HBV and HCV titers, and α-fetoprotein (AFP). Abdominal triphasic CT or MRI was performed for evaluation of the extent of HCC.

C-ion RT

The carbon ion beam used for radiotherapy was generated by the heavy ion medical accelerator in Chiba developed by NIRS in 1993. The accelerator system and the biophysical characteristics of the carbon ion beam have been previously described [13–15]. For modulation of the Bragg peak of the beam to conform to the target volume, the beam lines in the treatment room are equipped with a pair of wobbler magnets, beam scatterers, ridge filters, multileaf collimators, and a compensation bolus.

Before therapeutic planning, all patients had metallic markers (iridium seeds, 0.5 mm in diameter and 3 mm in length) implanted near the tumor to obtain precise treatment positioning. The irradiation fields were established with a three-dimensional therapy plan on the basis of 5-mm-thick CT images. The planning target volume was defined according to the shape of the tumor plus a 1.0–1.2 cm margin. To reproduce the target position accurately, a low-temperature thermoplastic sheet (Shellfitter, Kuraray, Osaka, Japan), a customized cradle (Moldcare, Alcare, Tokyo, Japan), and a respiratory gated irradiation system [34] were used in the CT planning and radiotherapy performance. The radiation field was confirmed and corrected by orthogonal fluoroscopy and radiography immediately before each treatment session.

Irradiation doses were expressed in Gray equivalents (GyE = carbon physical dose [in Gray] × relative biologic effectiveness). The relative biologic effectiveness value of carbon ions was assumed to be 3 at the distal part of the spread-out Bragg peak [35]. C-ion RT was given once daily, 4 days a week, for four fractions in 1 week. The dose per fraction was 13.2 GyE, so all patients received a total dose of 52.8 GyE.

Follow-up and evaluation criteria

All patients were assessed according to a predetermined schedule. After C-ion RT, patients were evaluated on the basis of physical examinations and blood tests once a month for the first year, once every 3 months for the following year, and once every 3–6 months thereafter. Contrast-enhanced CT or MRI was performed every 3 months for the first 2 years and every 6 months thereafter. Local control was defined as no sign of regrowth or new tumor in the treatment volume. Local recurrence was defined as failure of local control. Overall survival was measured from the starting date of treatment until the date of death from any cause. Cause-specific survival was defined as the interval between the starting date of treatment and the date of death from liver failure or HCC. Disease-free survival was defined as the interval between the starting date of treatment and the date of the diagnosis of the first recurrence or death from any cause. Acute and late toxicities were assessed using the National Cancer Institute Common Criteria, version 2.0, and the Radiation Therapy Oncology Group/European Organization for Research and Treatment of Cancer late radiation morbidity scoring scheme. Liver toxicity in late phase was assessed by Child-Pugh score, a commonly used marker of hepatic functional reserve in chronic liver disease.

Statistical analysis

Statistical analyses were performed using SPSS version 12.0 (SPSS Inc., Chicago, IL). For continuous variables, non-parametric tests (Mann–Whitney *U* test) were used. For categorical data, chi-squared test or Fisher's exact test was used. The Kaplan–Meier method was used for calculation of local control and survival rates, and the survival curves were compared by log-rank test. Statistical significance was considered if $P < 0.05$ (*P*-values from two-sided tests).

Results

There were no significant differences in sex, age, Child-Pugh classification, clinical stage, maximum tumor diameter, and tumor number between the two groups. The porta hepatis group exhibited greater vascular invasion than the non-porta hepatis group ($P = 0.066$).

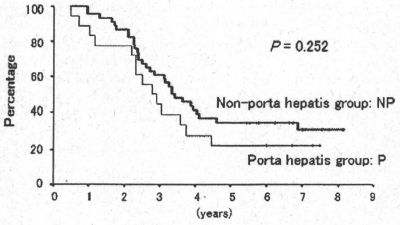

Number of patients at risk

NP	46	44	40	28	19	16	12	7	2	0
P	18	16	14	8	5	4	4	2	0	0

Fig. 1. Overall survival rate according to tumor localization. Overall survival rates after 3 and 5 years were 44.4% and 22.2% in the porta hepatis group and 60.9% and 34.8% in the non-porta hepatis group, respectively. There were no significant differences between the two groups ($P = 0.252$).

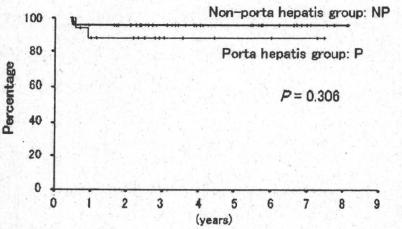

Number of patients at risk

NP	46	42	39	28	19	16	12	7	2	0
P	18	14	12	6	4	3	3	2	0	0

Fig. 2. Local control rate according to tumor localization. Local control rates after both 3 and 5 years were 87.8% in the porta hepatis group and 95.7% in the non-porta hepatis group. There were no significant differences between the two groups ($P = 0.306$).

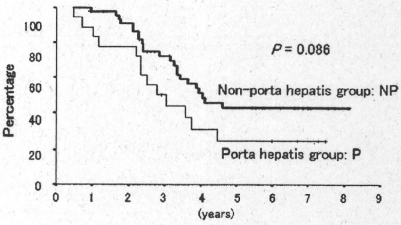

Number of patients at risk

NP	46	44	40	28	19	16	12	7	2	0
P	18	16	14	8	5	4	4	2	0	0

Fig. 3. Cause-specific survival rate according to tumor localization. Cause-specific survival rates after 3 and 5 years were 50.0% and 25.0% in the porta hepatis group and 72.3% and 42.8% in the non-porta hepatis group, respectively. The porta hepatis group showed a trend towards inferior outcome compared to the non-porta hepatis group ($P = 0.086$).

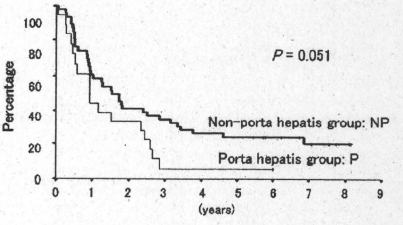

Number of patients at risk

NP	46	28	19	16	12	11	8	5	2	0
P	18	8	6	1	1	1	1	0	0	0

Fig. 4. Disease-free survival rate according to tumor localization. Disease-free survival rates after both 3 and 5 years were 5.6% in the porta hepatis group, and they were 34.8% and 23.9% in the non-porta hepatis group, respectively. The porta hepatis group showed a trend towards inferior outcome compared to the non-porta hepatis group ($P = 0.051$).

The median observation period for survival was 34 months (range, 6–90 months) in the porta hepatis group and 41 months (range, 11–98 months) in the non-porta hepatis group. Four patients were alive at last follow-up and 14 had died in the porta hepatis group, and 15 were alive at last follow-up and 31 had died in the non-porta hepatis group. Overall survival rates after 3 and 5 years were 44.4% [95% confidence interval (CI), 22–67] and 22.2% [95% CI, 3–41] in the porta hepatis group and 60.9% [95% CI, 47–75] and 34.8% [95% CI, 21–49] in the non-porta hepatis group, respectively (Fig. 1). Local control rates after both 3 and 5 years were 87.8% [95% CI, 72–104] in the porta hepatis group and 95.7% [95% CI, 90–102] in the non-porta hepatis group, respectively (Fig. 2). There were no significant differences between the two groups in overall survival and local control rates ($P = 0.252$, $P = 0.306$, respectively). Cause-specific survival rates after 3 and 5 years were 50.0% [95% CI, 27–73] and 25.0% [95% CI, 4–46] in the porta hepatis group and 72.3% [95% CI, 59–86] and 42.8% [95% CI, 27–58] in the non-porta hepatis group, respectively (Fig. 3). Disease-free survival rates after both 3 and 5 years were 5.6% [95% CI, −5 to 16] in the porta hepatis group, and they were 34.8% [95% CI, 21–49] and 23.9% [95% CI, 12–36] in the non-porta hepatis group, respectively (Fig. 4). In the cause-specific and disease-free survival rates, the porta hepatis group showed a trend towards inferior outcome compared to the non-porta hepatis group ($P = 0.086$, $P = 0.051$, respectively).

Toxicities in early phase are shown in Table 2. Adverse events of grade 3 or more were compared between the two groups. There were no significant differences in hepatic and hematologic toxicities ($P > 0.999$, $P = 0.190$, respectively). As to Child-Pugh score in late phase, cases with changes in Child-Pugh score within 1-point increase were 13 in the porta hepatis group and 41 in the non-porta hepatis group. Those with changes in score increasing by at least 2 points were five in each of the groups. There were no significant differences between the two groups in terms of change in Child-Pugh score (≤ 1 vs. ≥ 2) ($P = 0.128$) (Table 3). In terms of other non-hematologic toxicities such as skin and gastrointestinal toxicities, toxicities of grade 3 or higher did not occur. No patient had biliary stenosis associated with C-ion RT.

Table 2
Toxicities in early phase.

	Porta hepatis group Grade					Non-porta hepatis group Grade				
	0	1	2	3	4	0	1	2	3	4
Liver	2	4	9	3	0	7	15	16	8	0
Blood	6	2	4	6	0	13	9	16	8	0

There were no significant differences between porta hepatis and non-porta hepatis groups in liver and blood toxicities (grade 0–2 vs. grade 3–4) by Fisher's exact test. $P > 0.999$ (liver toxicity); $P = 0.190$ (blood toxicity).

Table 3
Change of Child-Pugh score in late phase.

	≤1	≥2
Porta hepatis group	13	5
Non-porta hepatis group	41	5

There were no significant differences between porta hepatis and non-porta hepatis groups in change of Child-Pugh score (≤1 vs. ≥2) by Fisher's exact test. $P = 0.128$.

Discussion

It is important that the treatment of HCC involves minimum invasiveness and complications in general. Surgical resection and RFA are essential curative therapies for HCC. In surgical resection, it was reported that both the 5-year overall survival and disease-free survival rates of the anatomic resection group were significantly better than those of the non-anatomic resection group, as HCC has a nature to cause intrahepatic metastasis via vascular invasion [36]. Anatomic resection consists of the systematic removal of a hepatic segment confined by tumor-bearing portal tributaries. In some patients with HCC adjacent to the porta hepatis, anatomic resection implies greater invasiveness because the resection volume becomes larger.

Concerning the use of RFA, puncture of the liver hilus, with the risk of injury to the portal vein or bile duct, presents a potentially dangerous scenario. It was reported that RFA was performed for patients with HCC adjacent to the porta hepatis under the condition of cooling the bile duct by endoscopic nasobiliary drainage tube to prevent biliary complications [31]. But the procedure is too complex to be a common therapy. Additionally, in cases of HCC with contiguous vessels, blood flow reduces the thermal effects of RFA, a phenomenon that increases the likelihood of the presence of residual viable tumor cells [37–39].

According to the above, we need to consider the degree of invasiveness and complications and carefully select an appropriate treatment modality because HCC adjacent to the porta hepatis is close to vessels and bile duct. In this study, therefore, differences in treatment effect and toxicities according to tumor localization, whether adjacent to the porta hepatis or not, were investigated retrospectively.

In the comparison of patient and tumor characteristics, the porta hepatis group demonstrated a trend towards a higher rate of vascular invasion compared to the non-porta hepatis group ($P = 0.066$). It is suggested that this was due to the tumor location.

Local control rates after 5 years were 87.8% [95% CI, 72–104] in the porta hepatis group and 95.7% [95% CI, 90–102] in the non-porta hepatis group. Thus, we obtained excellent local control rates in both groups. Local failure occurred in only four of all patients—two each in the porta hepatis and non-porta hepatis groups. There were no significant differences in toxicities. Biliary stenosis associated with C-ion RT did not occur in either group. Therefore, in certain patients with a higher risk of injury to the bile duct when undergoing RFA, in high-risk cases such as elderly patients for postoperative complications after surgical resection, or in some patients who refuse to undergo hepatectomy or RFA, C-ion RT appears to offer a promising therapeutic alternative for HCC.

However, cause-specific and disease-free survival rates after 5 years were 25.0% [95% CI, 4–46] and 5.6% [95% CI, −5 to 16] in the porta hepatis group and 42.8% [95% CI, 27–58] and 23.9% [95% CI, 12–36] in the non-porta hepatis group, respectively, which indicates a difference which is of borderline significance ($P = 0.086$, $P = 0.051$). The presence of vascular invasion is higher in the porta hepatis group ($P = 0.066$). A characteristic of HCC is the potential of causing intrahepatic metastasis via vascular invasion, and therefore the cause-specific and disease-free survival rates are mainly representing the rate of intrahepatic metastases/new tumors as there were almost no local failures (Fig. 2). This emphasizes the necessity to take into account the possibility of intrahepatic metastasis via vascular invasion. Of course, the importance of the earliest possible detection of a new tumor lesion and its treatment with an appropriate therapeutic modality cannot be overstated. In this regard, it is considered especially important to keep in mind the clinical multidisciplinary approach available for treating HCC.

As for radiation therapy for HCC adjacent to the porta hepatis, it was reported that proton beam therapy delivering 72.6 GyE in 22 fractions appears effective and safe. Overall 3-year survival and local control rates were 45.1% and 86.0%, respectively [40]. In our study, these rates in the porta hepatis group were 44.4% [95% CI, 22–67] and 87.8% [95% CI, 72–104], respectively. Therefore, the treatment effect of short-course C-ion RT is suggested to be almost equal to that of proton beam therapy with a more fractionated regimen.

A limitation of this study was the fact that the patient number in the porta hepatis group was small. It is therefore important to collect such cases and continuously verify efficacy and safety of short-course C-ion RT for patients with HCC adjacent to the porta hepatis.

In conclusion, excellent local control was achieved independent of tumor localization. There was no significant difference in treatment-related toxicity between the porta hepatis and non-porta hepatis groups. The short-course C-ion RT of 52.8 GyE in four fractions appears to be an effective and safe therapeutic option for porta hepatis patients just as it is for non-porta hepatis patients.

Conflict of interest statement

Any actual or potential conflicts of interest do not exist.

Acknowledgements

This study was supported by the Research Project with Heavy Ions of the National Institute of Radiological Sciences in Japan. We are grateful to the members of the National Institute of Radiological Sciences.

References

[1] Bosch FX, Ribes J, Borras J. Epidemiology of primary liver cancer. Semin Liver Dis 1999;19:271–85.
[2] Phillips R, Murakami K. Preliminary neoplasms of the liver. Results of radiation therapy. Cancer 1960;13:714–20.
[3] Stillwagon GB, Order SE, Guse C, et al. 194 Hepatocellular cancers treated by radiation and chemotherapy combinations: Toxicity and response: a Radiation Therapy Oncology Group study. Int J Radiat Oncol Biol Phys 1989;17:1223–9.
[4] Robertson JM, Lawrence TS, Dworzanin LM, et al. Treatment of primary hepatobiliary cancers with conformal radiation therapy and regional chemotherapy. J Clin Oncol 1993;11:1286–93.
[5] Toya R, Murakami R, Baba Y, et al. Conformal radiation therapy for portal vein tumor thrombosis of hepatocellular carcinoma. Radiother Oncol 2007;84:266–71.

[6] Xi M, Liu MZ, Deng XW, et al. Defining internal target volume (ITV) for hepatocellular carcinoma using four-dimensional CT. Radiother Oncol 2007;84:272–8.
[7] Zhao JD, Xu ZY, Zhu J, et al. Application of active breathing control in 3-dimensional conformal radiation therapy for hepatocellular carcinoma: the feasibility and benefit. Radiother Oncol 2008;87:439–44.
[8] Suit HD, Goitein M, Munzenrider J, et al. Increased efficacy of radiation therapy by use of proton beam. Strahlenther Onkol 1990;166:40–4.
[9] Matsuzaki Y, Osuga T, Saito Y, et al. A new, effective, and safe therapeutic option using proton irradiation for hepatocellular carcinoma. Gastroenterology 1994;106:1032–41.
[10] Matsuzaki Y. The efficacy of powerful proton radiotherapy for hepatocellular carcinoma-long term effects and QOL. Ann Cancer Res Ther 1998;7:9–17.
[11] Blakely EA, Ngo FQH, Curtis SB, et al. Heavy ion radiobiology: cellular studies. Adv Radiat Biol 1984;11:295–378.
[12] Castro JR. Future research strategy for heavy ion radiotherapy. In: Kogelnih HD, editor. Progress in radio-oncology. Bologna: Monduzzi Editore; 1995. p. 643–8.
[13] Sato K, Yamada H, Ogawa K, et al. Performance of HIMAC. Nucl Phys 1995;A588:229–34.
[14] Kanai T, Furusawa Y, Fukutsu K, Itsukaichi H, Eguchi-Kasai K, Ohara H. Irradiation of mixed beam and design of spread-out Bragg peak for heavy-ion radiotherapy. Radiat Res 1997;147:78–85.
[15] Kanai T, Endo M, Minohara S, et al. Biophysical characteristics of HIMAC clinical irradiation system for heavy-ion radiation therapy. Int J Radiat Oncol Biol Phys 1999;44:201–10.
[16] Tsujii H, Morita S, Miyamoto T, et al. Preliminary results of phase I/II carbon ion therapy. J Brachyther Int 1997;13:1–8.
[17] Kato H, Tsujii H, Miyamoto T, et al. Results of the first prospective study of carbon ion radiotherapy for hepatocellular carcinoma with liver cirrhosis. Int J Radiat Oncol Biol Phys 2004;59:1468–76.
[18] Tsujii H, Mizoe JE, Kamada T, et al. Overview of clinical experiences on carbon ion radiotherapy at NIRS. Radiother Oncol 2004;73:S41–49.
[19] Kato H, Yamada S, Yasuda S, et al. Phase II study of short-course carbon ion radiotherapy (52.8 GyE/4-fraction/1-week) for hepatocellular carcinoma. Hepatology 2005;42:381A.
[20] Ikai I, Arii S, Okazaki M, et al. Report of the 17th nationwide follow-up survey of primary liver cancer in Japan. Hepatol Res 2007;37:676–91.
[21] Mulcahy MF. Management of hepatocellular cancer. Curr Treat Options Oncol 2005;6:423–35.
[22] Mazzaferro V, Regalia E, Doci R, et al. Liver transplantation for the treatment of small hepatocellular carcinomas in patients with cirrhosis. N Engl J Med 1996;334:693–9.
[23] Llovet JM, Fuster J, Bruix J. Intention-to-treat analysis of surgical treatment for early hepatocellular carcinoma: resection versus transplantation. Hepatology 1999;30:1434–40.
[24] Yoo HY, Patt CH, Geschwind JF, et al. The outcome of liver transplantation in patients with hepatocellular carcinoma in the United States between 1988 and 2001: 5-year survival has improved significantly with time. J Clin Oncol 2003;21:4329–35.
[25] Kuvshinoff BW, Ota DM. Radiofrequency ablation of liver tumors: influence of technique and tumor size. Surgery 2002;132:605–11.
[26] Shiina S, Teratani T, Obi S, et al. A randomized controlled trial of radiofrequency ablation with ethanol injection for small hepatocellular carcinoma. Gastroenterology 2005;129:122–30.
[27] Sato M, Watanabe Y, Ueda S, et al. Microwave coagulation therapy for hepatocellular carcinoma. Gastroenterology 1996;110:1507–14.
[28] Patterson EJ, Scudamore CH, Owen DA, et al. Radiofrequency ablation of porcine liver in vivo: effects of blood flow and treatment time on lesion size. Ann Surg 1998;227:559–65.
[29] Livraghi T, Solbiati L, Meloni MF, et al. Treatment of focal liver tumors with percutaneous radio-frequency ablation: complications encountered in a multicenter study. Radiology 2003;226:441–51.
[30] Nakazawa T, Kokubu S, Shibuya A, et al. Radiofrequency ablation of hepatocellular carcinoma: correlation between local tumor progression after ablation and ablative margin. AJR Am J Roentgenol 2007;188:480–8.
[31] Ohnishi T, Yasuda I, Nishigaki Y, et al. Intraductal chilled saline perfusion to prevent bile duct injury during percutaneous radiofrequency ablation for hepatocellular carcinoma. J Gastroenterol Hepatol 2008;23:e410–415.
[32] Llovet JM, Bru C, Bruix J. Prognosis of hepatocellular carcinoma: the BCLC staging classification. Semin liver Dis 1999;19:329–38.
[33] Llovet JM, Burroughs A, Bruix J. Hepatocellular carcinoma. Lancet 2003;362:1907–17.
[34] Minohara S, Kanai T, Endo M, Noda K, Kanazawa M. Respiratory gated irradiation system for heavy-ion radiotherapy. Int J Radiat Oncol Biol Phys 2000;47:1097–103.
[35] Suzuki M, Kase Y, Yamaguchi H, Kanai T, Ando K. Relative biological effectiveness for cell-killing effect on various human cell lines irradiated with heavy-ion medical accelerator in Chiba (HIMAC) carbon-ion beams. Int J Radiat Oncol Biol Phys 2000;48:241–50.
[36] Hasegawa K, Kokudo N, Imamura H, et al. Prognostic impact of anatomic resection for hepatocellular carcinoma. Ann Surg 2005;242:252–9.
[37] Rossi S, Garbagnati F, Lencioni R, et al. Percutaneous radio-frequency thermal ablation of nonresectable hepatocellular carcinoma after occlusion of tumor blood supply. Radiology 2000;217:119–26.
[38] McGhana JP, Dodd 3rd GD. Radiofrequency ablation of the liver: current status. AJR Am J Roentgenol 2001;176:3–16.
[39] de Baere T, Denys A, Wood BJ, et al. Radiofrequency liver ablation: experimental comparative study of water-cooled versus expandable systems. AJR Am J Roentgenol 2001;176:187–92.
[40] Mizumoto M, Tokuuye K, Sugahara S, et al. Proton beam therapy for hepatocellular carcinoma adjacent to the prota hepatis. Int J Radiat Oncol Biol Phys 2008;71:462–7.

Radiotherapy and Oncology 96 (2010) 236–242

Contents lists available at ScienceDirect

Radiotherapy and Oncology

journal homepage: www.thegreenjournal.com

Particle beam radiotherapy

Compensatory enlargement of the liver after treatment of hepatocellular carcinoma with carbon ion radiotherapy – Relation to prognosis and liver function

Hiroshi Imada [a,b,*], Hirotoshi Kato [a], Shigeo Yasuda [a], Shigeru Yamada [a], Takeshi Yanagi [a], Ryusuke Hara [a], Riwa Kishimoto [a], Susumu Kandatsu [a], Shinichi Minohara [a], Jun-etsu Mizoe [a], Tadashi Kamada [a], Osamu Yokosuka [b], Hirohiko Tsujii [a]

[a] Research Center for Charged Particle Therapy, National Institute of Radiological Sciences, Chiba, Japan; [b] Department of Medicine and Clinical Oncology, Graduate School of Medicine, Chiba University, Chiba, Japan

ARTICLE INFO

Article history:
Received 30 December 2008
Received in revised form 3 December 2009
Accepted 18 March 2010
Available online 21 April 2010

Keywords:
Hepatocellular carcinoma
Radiotherapy
Carbon ion
Liver volume
Liver function

ABSTRACT

Background and purpose: To examine whether liver volume changes affect prognosis and hepatic function in patients treated with carbon ion radiotherapy (CIRT) for hepatocellular carcinoma (HCC).

Material and methods: Between April 1995 and March 2003, among the cases treated with CIRT, 43 patients with HCC limited to the right hepatic lobe were considered eligible for the study. The left lateral segment was defined as the non-irradiated region. Liver volume was measured using contrast CT at 0, 3, 6, and 12 months after CIRT. We examined serum albumin, prothrombin activity, and total bilirubin level as hepatic functional reserve.

Results: After CIRT, the non-irradiated region showed significant enlargement, and enlarged volume of this region 3 months after CIRT $\geqslant 50\ cm^3$ was a prognostic factor. The 5-year overall survival rates were 48.9% in the larger enlargement group (enlarged volume of non-irradiated region 3 months after CIRT $\geqslant 50\ cm^3$) and 29.4% in the smaller enlargement group (as above, $<50\ cm^3$). The larger enlargement group showed better hepatic functional reserve than the smaller enlargement group 12 months after CIRT.

Conclusions: This study suggests that compensatory enlargement in the non-irradiated liver after CIRT contributes to the improvement of prognosis.

 Radiotherapy and Oncology 96 (2010) 236–242

Hepatocellular carcinoma (HCC) is one of the most common malignant tumors in the world and is the third-leading cause of death from cancer [1]. In Japan, its incidence is approximately 30 in 100,000 males and 10 in 100,000 females [2]. HCC is closely associated with hepatitis B and C, and the majority of patients with HCC have liver cirrhosis, a condition that limits treatment options. Surgical resection is the mainstay of curative treatment, but it is restricted to selected patients [3,4]. Radiofrequency ablation and other ablative techniques achieve excellent local control, but they are restricted to small HCC [5–7]. Transcatheter arterial chemoembolization is clinically useful [8–10], but a radical effect has not been proved in histopathologic studies [11,12]. There is an urgent need for more effective and less invasive treatment of HCC.

The previous role of radiotherapy for HCC was limited and unsatisfactory by poor hepatic tolerance to irradiation [13,14]. Technological advances have made it possible to deliver a higher dose of radiation to focal liver cancers accurately, reducing the risk of toxicity [15–17]. Proton beam therapy has appeared to be effective and safe for HCC, mainly because of its excellent dose distribution at the end of the beam path, called the Bragg peak [18,19]. Carbon ion beams also possess the Bragg peak, and they provide excellent dose localization to the target volume by specified beam modulations [20,21]. They have advantageous biological and physical properties that result in a higher cytocidal effect than those of photons and protons [22–27].

The history of the use of carbon ion radiotherapy (CIRT) for treating HCC goes back to 1995, when clinical trials were initiated at the National Institute of Radiological Sciences (NIRS). We have already reported that CIRT used for the treatment of HCC is safe and effective, and that it causes only minor liver damage [22,23]. Although atrophy of the irradiated region of the liver is observed after CIRT, the reason why liver function is retained after CIRT has not yet been investigated.

It has been reported that preoperative portal vein embolization in extended hepatectomy cases causes the remnant liver volume to increase and postoperative hepatic insufficiency to diminish [28,29]. Similarly, we wondered whether the same mechanism might apply to CIRT. Thus, as the region irradiated with CIRT showed atrophy and the non-irradiated region appeared to show

* Corresponding author at: Research Center for Charged Particle Therapy, National Institute of Radiological Sciences, 4-9-1, Anagawa, Inage-ku, Chiba 263-8555, Japan.
E-mail address: h_imada@nirs.go.jp (H. Imada).

0167-8140/$ - see front matter © 2010 Elsevier Ireland Ltd. All rights reserved.
doi:10.1016/j.radonc.2010.03.025

compensatory enlargement after CIRT, it was supposed that the compensatory enlargement had a contributory role in the retention of hepatic function. This hypothesis was investigated.

Materials and methods

Patients

CIRT for HCC was performed as a Phase I/II clinical trial from April 1995 through March 2001 with 110 patients, and as a Phase II clinical trial from April 2001 through March 2003 with 47 patients. The eligibility criteria for enrollment in these clinical trials were previously reported [22]. Prior to treatment, all patients gave their written informed consent in accordance with the Declaration of Helsinki. One hundred twenty-one of the total 157 had the tumor limited to the right lobe of the liver, 27 had the tumor limited to the left lobe, and 9 had the tumor in both right and left lobes.

Among the patients of this study, 43 met the following conditions: (1) treatment target tumor was limited to the right lobe of the liver, (2) left lateral segment was not irradiated, (3) no additional treatment was performed for hepatic lesions (local recurrence and/or recurrence in other loci) within 12 months after CIRT, and (4) abdominal contrast CT imaging was performed at our institute at 0, 3, 6 and 12 months after CIRT. Background data of the patients and tumors are presented in Table 1. The regions irradiated with more than 10% radiation dose were as follows: anterior, posterior and medial segments in 32 patients, anterior and posterior segments in 8, posterior segment in 2, and anterior and medial segments in 1.

Carbon ion radiotherapy

The carbon ion beam used for radiotherapy was generated from the heavy ion medical accelerator in Chiba developed by NIRS in 1993. The accelerator system and the biophysical characteristics of the carbon ion beam have been previously described [20,21,30]. For modulation of the Bragg peak of the beam to conform to the target volume, the beam lines in the treatment room are equipped with a pair of wobbler magnets, beam scatterers, ridge filters, multileaf collimators, and a compensation bolus. The irradiation fields were established with a three-dimensional therapy plan on the basis of 5-mm-thick CT images. The planning target volume was defined according to the shape of the tumor plus a 1.0–1.2 cm margin. To reproduce the target position accurately, a low-temperature thermoplastic sheet (Shellfitter, Kuraray, Osaka, Japan), a customized cradle (Moldcare, Alcare, Tokyo, Japan), and a respiratory gated irradiation system [31] were used in the CT planning and radiotherapy stages. The radiation field was confirmed and corrected by orthogonal fluoroscopy and radiography immediately before each treatment session.

Table 1
Patient and tumor characteristics.

	Total	Larger enlargement group	Smaller enlargement group	*P*
n	43	20	23	
Gender, n (%)				
Male	29 (67)	15 (75)	14 (61)	0.353
Female	14 (33)	5 (25)	9 (39)	
Age (years)				
Median	66	71.5	65	0.006
Range	45–83	46–81	45–83	
Child-Pugh classification, n (%)				
A	35 (81)	18 (90)	17 (74)	0.250
B	8 (19)	2 (10)	6 (26)	
Stage (UICC 5th), n (%)				
I	13 (32)	6 (27)	7 (36)	0.947
II	25 (54)	12 (59)	13 (50)	
IIIA	5 (14)	2 (14)	3 (14)	
Gross tumor volume (cm^3)				
Median	35.2	54.7	31.8	0.114
Range	4.6–861.9	15.6–861.9	4.6–211.2	
Planning target volume (cm^3)				
Median	190.5	242.9	149.0	0.019
Range	39.6–1466.4	70.3–1466.4	39.6–538	
Liver volume of irradiated site (cm^3), mean ± SD	756.6 ± 134.1	767.1 ± 138.1	747.5 ± 132.9	0.942
Liver volume of non-irradiated site (cm^3), mean ± SD	320.0 ± 166.3	317.2 ± 152.7	322.4 ± 180.6	0.715
Albumin (g/dl), mean ± SD	3.8 ± 0.4	3.9 ± 0.4	3.8 ± 0.4	0.659
Prothrombin activity (%), mean ± SD	77.2 ± 13.5	78.6 ± 11.4	76.0 ± 15.3	0.670
Total bilirubin (mg/dl), mean ± SD	1.0 ± 0.4	0.9 ± 0.3	1.1 ± 0.4	0.072
Platelet count ($\times 10^4/\mu l$), mean ± SD	11.8 ± 4.6	14.0 ± 4.3	9.9 ± 3.9	0.002
Number of tumors, n (%)				
1	36 (84)	19 (95)	17 (74)	0.100
2	7 (16)	1 (5)	6 (26)	
Irradiated segment, n (%)				
Anterior, posterior and medial	32	15	17	0.821
Anterior and posterior	8	4	4	
Posterior	2	1	1	
Anterior and medial	1	0	1	
Number of portals, n (%)				
2	36	16	20	0.687
3	7	4	3	

Abbreviations: UICC = International Union Against Cancer.
SD = standard deviation.

Table 2
Dose fractionation.

Total dose/ fractionation	Total (n = 43)	Larger enlargement group (n = 20)	Smaller enlargement group (n = 23)	BED (α/β = 10)
49.5 GyE/15 fr	1	1	0	65.8
54.0 GyE/15 fr	1	0	1	73.4
60.0 GyE/15 fr	2	0	2	84.0
66.0 GyE/15 fr	2	1	1	95.0
72.0 GyE/15 fr	3	1	2	106.6
79.5 GyE/15 fr	1	0	1	121.6
54.0 GyE/12 fr	1	0	1	78.3
60.0 GyE/12 fr	3	2	1	90.0
66.0 GyE/12 fr	2	2	0	102.3
69.6 GyE/12 fr	4	1	3	110.0
48.0 GyE/8 fr	2	0	2	76.8
52.8 GyE/8 fr	7	3	4	87.6
52.8 GyE/4 fr	14	9	5	122.5

Abbreviations: BED = biological effective dose.

The dose was calculated for the target volume and any nearby critical structures and expressed in Gray equivalents (GyE = carbon physical dose [in Gray] × relative biologic effectiveness). Radiobiologic studies were performed in mice and in five human cell lines cultured *in vitro* to estimate the relative biologic effectiveness values relative to megavoltage photons. Irrespective of the size of the spread-out Bragg peak (SOBP), the relative biologic effectiveness value of carbon ions was estimated as 3.0 at the distal part of the SOBP, and ridge filters were designed to produce a physical dose gradient of the SOBP so that the biologic effect along the SOBP became uniform. This was based on the biologic response of human salivary gland tumor cells at a 10% survival level.

CIRT was given at a total dose range of 48.0–79.5 GyE in 4–15 fractions. Ten patients were treated at a total dose range of 49.5–79.5 GyE in 15 fractions, 10 at 54.0–69.6 GyE in 12 fractions, 9 at 48.0–52.8 GyE in 8 fractions, and 14 at 52.8 GyE in four fractions. CIRT was administered once a day, four fractions per a week, and one port was used in each session. Double-field geometry was used for CIRT in 36 patients; for the remaining seven patients, three-field geometry was used (Tables 1 and 2).

Measurement of liver volume

The left lateral segment of the liver was defined as the non-irradiated region, and the other segments as irradiated. The AZE Company Workstation VIRTUAL PLACE ADVANCE PLUS liver analysis software was used for measuring liver volume. Liver contours (both irradiated and non-irradiated regions) and contours of the target tumors to be treated were entered on each of the CT slices taken prior to treatment and at 3, 6 and 12 months after CIRT, and the volume of the liver in the irradiated region (excluding the target tumor volume) as well as that in the non-irradiated region were measured. Since hepatic cirrhosis is noted in most cases as the background disease, and to exclude any impact of right lobe atrophy and left lobe enlargement through natural processes, the evaluation period was limited to 12 months after treatment.

Survival and evaluation of liver function

Overall survival was measured from the starting date of treatment until the date of death from any cause. Disease-free survival was measured from the starting date of treatment to the time of either death due to disease or of the first clinical or radiographic evidence of systemic or regional disease recurrence. We investigated the relationships between survivals and enlargement volume of the non-irradiated region at 3 months after CIRT. Patients with 50 cm^3 or greater enlargement volume of the non-irradiated region at 3 months post-treatment were classified as the larger enlargement group, and those with less than 50 cm^3 enlargement as the smaller enlargement group. Serial changes in serum albumin, prothrombin activity, total bilirubin level, and platelet count were reviewed before and 12 months after treatment in the larger and smaller enlargement groups.

Statistical analysis

Statistical analyses were performed using SPSS version 12.0 (SPSS Inc., Chicago, IL). Results were reported as mean ± standard deviation. For continuous variables, non-parametric tests (Friedman test, Wilcoxon's signed r rank test, and Mann–Whitney U test) were used. For categorical data, chi-squared test or Fisher's exact test was used. Prognostic factor analyses were performed using the Cox proportional hazards regression model. The Kaplan–Meier method was used for calculation of survival rates, and survival curves were compared by log-rank test. Multivariate analyses of factors related to enlargement of the non-irradiated region at 3 months after CIRT were performed using logistic regression analyses. Statistical significance was considered if $P < 0.05$ (P-values from two-sided tests), but for multiple comparisons of liver volume, Bonferroni's inequality was used.

Table 3
Changes in liver volume.

	Before	3 months after	6 months after	12 months after
Total (n = 43)				
Irradiated region (cm^3)	756.6 ± 134.1	696.1 ± 229.1	632.9 ± 164.2	575.9 ± 145.7
Volume variation (cm^3) (%)	−60.5 ± 204.3 (−7.8 ± 28.1)	−123.7 ± 145.7 (−15.9 ± 19.0)	−180.7 ± 104.2 (−24.0 ± 13.7)	
Non-irradiated region (cm^3)	320.0 ± 166.3	379.4 ± 169.4	389.5 ± 177.5	390.4 ± 185.7
Volume variation (cm^3) (%)	59.4 ± 80.4 (25.3 ± 37.2)	69.5 ± 85.3 (28.7 ± 36.6)	70.4 ± 85.2 (27.0 ± 33.9)	
Larger enlargement group (n = 20)				
Irradiated region (cm^3)	767.1 ± 138.1	726.7 ± 294.5	662.8 ± 178.8	582.7 ± 149.3
Volume variation (cm^3) (%)	−40.4 ± 279.8 (−4.7 ± 39.1)	−104.3 ± 177.7 (−12.7 ± 23.8)	−184.4 ± 111.9 (−24.1 ± 15.3)	
Non-irradiated region (cm^3)	317.2 ± 152.7	438.1 ± 152.0	444.9 ± 165.0	441.9 ± 162.7
Volume variation (cm^3) (%)	120.9 ± 74.1 (47.7 ± 42.6)	127.7 ± 84.0 (50.3 ± 40.5)		
Smaller enlargement group (n = 23)				
Irradiated region (cm^3)	747.5 ± 132.9	669.4 ± 154.1	606.9 ± 149.4	570.0 ± 145.7
Volume variation (cm^3) (%)	−78.1 ± 106.6 (−10.4 ± 13.2)	−140.6 ± 112.3 (−18.7 ± 13.6)	−177.5 ± 99.4 (−24.0 ± 12.4)	
Non-irradiated region (cm^3)	322.4 ± 180.6	328.3 ± 170.2	341.3 ± 177.3	345.6 ± 196.1
Volume variation (cm^3)(%)	5.9 ± 34.0 (5.8 ± 15.2)	18.9 ± 45.2 (10.0 ± 18.8)	23.2 ± 60.1 (9.6 ± 20.6)	

Values are given as mean ± standard deviation.

Results

The changes with time in liver volume values are shown in Table 3. In all patients, the volume of the irradiated region decreased significantly and that of the non-irradiated region increased significantly by the Friedman test ($P < 0.001$, $P < 0.001$, respectively), with the difference over time in the irradiated region by multiple comparisons showing that significant differences existed between any two time-points ($P < 0.001$, each). In the non-irradiated region, comparisons showed that significant differences existed between before treatment and 3, 6, and 12 months after treatment ($P < 0.001$, $P < 0.001$, $P < 0.001$, respectively), but there were no significant differences between 3 and 6 months, 3 and 12 months, and 6 and 12 months ($P = 0.091$, $P = 0.084$, and $P = 0.599$, respectively). Comparing the time-related changes of the liver volume in terms of the larger and smaller enlargement groups, both of the two groups showed significant atrophy of the irradiated region ($P < 0.001$, $P < 0.001$, respectively) and significant enlargement of the non-irradiated region ($P < 0.001$, $P = 0.022$, respectively) (Fig. 1). Further, the enlarged volume of the non-irradiated region 3 months after CIRT $\geqslant 50$ cm^3 was a prognostic factor (Table 4).

There were significant differences between the larger and smaller enlargement groups in overall survival rate and disease-free survival rate ($P = 0.030$, $P = 0.008$, respectively). Overall survival rates after 3 and 5 years were 80.0% (95% confidence interval [CI], 63–98) and 48.9% (95% CI, 27–71) in the larger enlargement group and 52.2% (95% CI, 32–73) and 29.4% (95% CI, 10–48) in the smaller enlargement group (Fig. 2a). Disease-free survival rates after 3 and 5 years were 50.0% (95% CI, 28–72) and 28.0% (95% CI, 7–49) in the larger enlargement group and 26.1% (95% CI, 8–44) and 0.0% (95% CI, 0–0) in the smaller enlargement group (Fig. 2b).

Table 5 shows the comparison of liver function between the two groups. Before treatment, there were no significant differences in serum albumin, prothrombin activity, and total bilirubin level between the two groups ($P = 0.659$, $P = 0.670$, and $P = 0.072$, respectively). Yet, 12 months after the treatment the larger enlargement group exhibited significantly higher serum albumin and prothrombin activity and lower total bilirubin levels than the smaller enlargement group ($P = 0.015$, $P = 0.002$, $P = 0.042$, respectively). As for platelet count, there were significant differences between the two groups before and after the treatment ($P = 0.002$, $P = 0.002$, respectively).

Univariate analysis showed that the planning target volume (PTV) and platelet count were significant factors for compensatory liver enlargement. Multivariate analysis showed only platelet count to be a significant factor (Table 6).

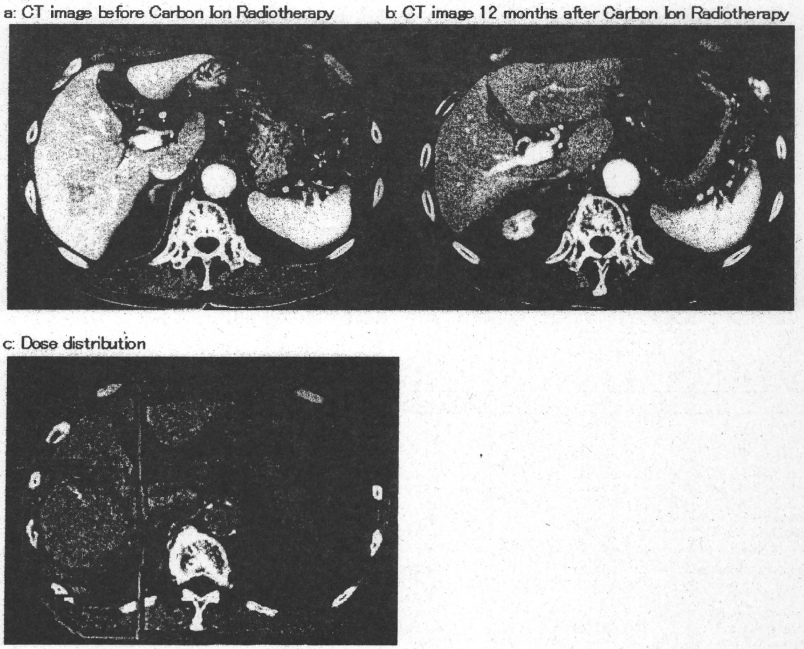

Fig. 1. CT images before and 12 months after carbon ion radiotherapy and dose distribution. CT image obtained in 81-year-old man from the larger enlargement group shows shrinkage of right hepatic lobe (840.5 cm^3 → 739.0 cm^3) and enlargement of left lateral segment (154.5 cm^3 → 266.4 cm^3). Hepatic function of this patient was retained. Serum albumin level before and 12 months after therapy was 4.5 and 4.0 g/dl, respectively. Prothrombin activity was 85.7% and 82.7%, respectively. Total bilirubin level was 0.7 and 0.7 mg/dl, respectively. Platelet count was 13.5×10^4 and $17.8 \times 10^4/\mu$l, respectively.

Table 4
Factors related to overall survival.

Factor	No. of patients	Univariate		Multivariate	
		Hazard ratio (95% CI)	P	Hazard ratio (95% CI)	P
Gender					
Male	29	1.00 (0.47–2.10)	0.994	0.55 (0.18–1.72)	0.305
Female	14				
Age (years)					
<65	15	1.12 (0.59–2.43)	0.614	1.82 (0.80–4.18)	0.155
⩾65	28				
Child-Pugh classification					
A	35	1.40 (0.63–3.10)	0.406	1.48 (0.45–4.85)	0.520
B	8				
Platelet count ($\times 10^4/\mu l$)					
<10	17	0.57 (0.29–1.15)	0.114	0.51 (0.20–1.33)	0.169
⩾10	26				
Enlargement volume of non-irradiated region at 3 months after CIRT (cm^3)					
<50	23	0.45 (0.22–0.94)	0.034	0.36 (0.15–0.88)	0.025
⩾50	20				
Planning target volume (cm^3)					
<200	24	0.78 (0.39–1.56)	0.489	1.51 (0.63–3.59)	0.357
⩾200	19				
Biological effective dose (α/β = 10)					
Low (65.8–95.0)	19	0.81 (0.41–1.62)	0.555	0.95 (0.41–2.20)	0.912
High (102.3–122.5)	24				
Number of tumors					
1	36	1.07 (0.44–2.61)	0.881	0.50 (0.16–1.54)	0.226
2	7				

Discussion

In the present study, we have shown that cases with irradiation of the right lobe of the liver develop enlargement of the left lateral segment by way of compensation after CIRT and that the compensatory enlargement is contributory to the improvement of prognosis.

Approximately 80% of all HCC patients have chronic liver disorders [3], which require effective and necessarily minimally invasive therapy of HCC. We have reported that CIRT appears safe and effective for patients with HCC [22,23]. However, the reason why liver function is retained despite atrophy of the irradiated region of the liver still remained to be investigated. Hemming et al. reported that preoperative portal vein embolization performed in extended hepatectomy cases caused enlargement of the remnant liver [28]. In other research studies, enlargement of the remnant liver has been shown to have the effect of improving liver function [32–34]. Moreover, after radiotherapy, veno-occlusive diseases of the liver occur, which, it is argued, are the cause of radiation-induced liver disease [35–37]. From the above, we wonder whether the same mechanism might hold true for CIRT.

In this study, we measured the volumes of the irradiated and non-irradiated regions using CT imaging. Heymsfield and associates first measured the volume of a cadaver's liver using CT in 1979, showing that the discrepancy between the volume measured by CT and that measured using the water replacement method was

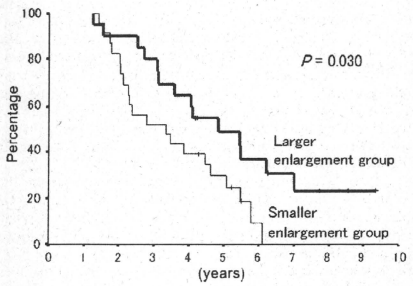

Fig. 2a. Survival rates of the larger and smaller enlargement groups. (a) Overall survival of the larger and smaller enlargement groups. Overall survival rates after 3 and 5 years were 80.0% (95% confidence interval [CI], 63–98) and 48.9% (95% CI, 27–71) in the larger enlargement group and 52.2% (95% CI, 32–73) and 29.4% (95% CI, 10–48) in the smaller enlargement group.

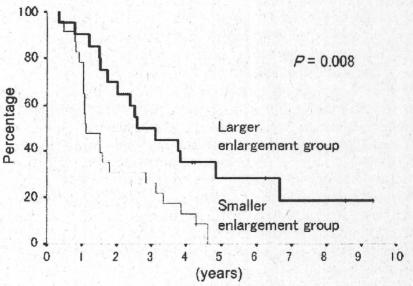

Fig. 2b. Survival rates of the larger and smaller enlargement groups. (b) Disease-free survival of the larger and smaller enlargement groups. Disease-free survival rates after 3 and 5 years were 50.0% (95% CI, 28–72) and 28.0% (95% CI, 7–49) in the larger enlargement group and 26.1% (95% CI, 8–44) and 0.0% (95% CI, 0–0) in the smaller enlargement group.

Table 5
Comparison of liver function.

	Before			12 months after		
	Larger enlargement group ($n = 20$)	Smaller enlargement group ($n = 23$)	P	Larger enlargement group ($n = 20$)	Smaller enlargement group ($n = 23$)	P
Albumin (g/dl)	3.9 ± 0.4	3.8 ± 0.4	0.659	3.9 ± 0.3	3.7 ± 0.4	0.015
Prothrombin activity (%)	78.6 ± 11.4	76.0 ± 15.3	0.670	81.9 ± 9.3	69.7 ± 11.9	0.002
Total bilirubin (mg/dl)	0.9 ± 0.3	1.1 ± 0.4	0.072	0.9 ± 0.5	1.1 ± 0.4	0.042
Platelet count ($\times 10^4$/μl)	14.0 ± 4.3	9.9 ± 3.9	0.002	14.6 ± 7.9	8.5 ± 3.4	0.002

Values are given as mean ± standard deviation.

Table 6
Factors related to compensatory enlargement.

Factor	No. of patients	Univariate P	Multivariate P	Hazard ratio	95% Confidence interval
Planning target volume (PTV) (cm^3)					
<200	24	0.013	0.147	2.92	0.69–12.46
⩾200	19				
Platelet count ($\times 10^4/\mu l$)					
<10	17	0.004	0.028	5.85	1.21–28.31
⩾10	26				
Biological effective dose (BED) ($\alpha/\beta = 10$)					
Low (65.8–95.0)	19	0.261	0.479	1.67	0.40–6.94
High (102.3–122.5)	24				

within 5% [38]. In 1981, Moss et al. also measured liver volume using CT, confirming the conclusion of Heymsfield et al. [39]. Many studies have reported that the difference between CT-measured liver volume and the actual liver volume is minor [38–40]. In our study, the volume of the left lateral segment was 320.0 ± 166.3 cm^3 (Table 3). Zhou et al. measured the volume of 113 hepatic lobes using CT. They reported average volumes of the left lateral segment of 313.2 ± 105.1 and 282.2 ± 136.2 cm^3 in Child-Pugh class A and B patients, respectively [41]. These results generally resemble ours, lending support to the accuracy and reliability of our measuring method.

It is difficult to distinguish strictly the irradiated and non-irradiated portions, and therefore in this study we defined the left lateral segment of the liver as the non-irradiated region, and the other segments as irradiated. In 11 of 43 patients, the region considered as irradiated was larger than the region really receiving radiation. We cannot examine whether the non-irradiated portions of the right lobes enlarge or not because it is difficult to distinguish the irradiated and non-irradiated portions of the right lobe. The volumes of the irradiated part of the liver measured at 0, 3, 6, and 12 months after treatment, respectively, did show significant differences. With the lapse of time, the measurement values decreased significantly. In contrast, the liver volumes of the non-irradiated part increased at 3 months post-treatment on a significant scale compared to before the treatment. From then on, no more significant increases were observed. These data demonstrate that the enlargement of the non-irradiated region is not a matter of the natural course associated with chronic liver disorders, but rather results as compensation for the CIRT-caused atrophy of the liver.

We divided the subjects into two groups according to compensatory enlargement liver volume of more or less than 50 cm^3 because enlarged volume of the non-irradiated region 3 months after CIRT ⩾50 cm^3 was a prognostic factor. In terms of liver function, many complex methods for estimating liver functional reserve have been advocated, including tests that measure liver metabolic activity such as ICG clearance, galactose elimination, and aminopyrine clearance [42]. However, it was demonstrated that either one of Child classification [43] or Okuda staging [44] is highly predictive for outcome [45]. Serum albumin, prothrombin activity, and total bilirubin level are the serum items of the Child-Pugh score, which is the index of hepatic functional reserve. Therefore, Serial changes in these items were reviewed as hepatic functional reserve before and 12 months after treatment in the two groups. There were no significant differences in them before the treatment, but at 12 months after, the larger enlargement group remained significantly more favorable than the smaller enlargement group. On the other hand, the extent of atrophy of the irradiated regions was found to be significantly similar in the two groups. These data indicate the possibility that the compensatory enlargement, taking place in the non-irradiated region of the liver after CIRT, affect hepatic functional reserve. It was suggested that better disease-free survival and hepatic functional reserve contributed to improvement of overall survival.

We investigated PTV, platelet count, and biological effective dose (BED) as indicators of enlargement of the non-irradiated region at 3 months after CIRT. PTV and platelet count were selected on the basis of their significant differences between the larger and smaller enlargement groups. In our study, it was difficult to compare the differences of total dose and fractionations because of their various combinations. Then, although it has not been confirmed that BED is adaptable to CIRT, we tried to calculate BED for every fractionation by L/Q model [46], adding it to the variables. The difference in mean age between the two groups was thought not to be related to the compensatory enlargement of the liver after CIRT, based on the self-evident discrepancy between age and the enlargement volume, i.e., the higher the age, the larger the volume. Therefore, we excluded age from the analysis of the indicators of compensatory enlargement of the non-irradiated liver. Our data demonstrated platelet count to be the major factor of compensatory enlargement of the non-irradiated liver, and it is known that platelet count decreases in parallel with the grade of chronic liver disease [47]. Thus, we intend to investigate the relationship between liver fibrosis and compensatory enlargement of the liver in future studies.

Considering the limitations of this study, we must first point out the nature of the investigation as a retrospective one. Secondly, the subjects were restricted to cases in which target tumors were located in the right lobe of the liver. Thirdly, we did not utilize any biochemical or molecular biological method.

It was demonstrated that the non-irradiated region of the liver enlarged compensatively until 3 months after CIRT and that the enlarged volume of this region 3 months after CIRT ⩾50 cm^3 was a prognostic factor. We can conclude that compensatory enlargement of the non-irradiated liver contributes to the improvement of prognosis.

Conflict of interest statement

Any actual or potential conflicts of interest do not exist.

Acknowledgments

This study was supported by the Research Project with Heavy Ions of the National Institute of Radiological Sciences in Japan. We are grateful to members of the National Institute of Radiological Sciences. We are indebted to Dr. Gen Kobashi and Dr. Kaori Ohta for statistical support.

References

[1] Bosch FX, Ribes J, Borras J. Epidemiology of primary liver cancer. Semin Liver Dis 1999;19:271–85.
[2] Marugame T, Matsuda T, Kamo K, et al. Cancer incidence and incidence rates in Japan in 2001 based on the data from 10 population-based cancer registries. Jpn J Clin Oncol 2007;37:884–91.
[3] Ikai I, Arii S, Okazaki M, et al. Report of the 17th Nationwide Follow-up Survey of Primary Liver Cancer in Japan. Hepatol Res 2007;37:676–91.
[4] Mulcahy MF. Management of hepatocellular cancer. Curr Treat Options Oncol 2005;6:423–35.
[5] Kuvshinoff BW, Ota DM. Radiofrequency ablation of liver tumors: influence of technique and tumor size. Surgery 2002;132:605–11.
[6] Shiina S, Teratani T, Obi S, et al. A randomized controlled trial of radiofrequency ablation with ethanol injection for small hepatocellular carcinoma. Gastroenterology 2005;129:122–30.
[7] Sato M, Watanabe Y, Ueda S, et al. Microwave coagulation therapy for hepatocellular carcinoma. Gastroenterology 1996;110:1507–14.
[8] Camma C, Schepis F, Orlando A, et al. Transarterial chemoembolization for unresectable hepatocellular carcinoma: meta-analysis of randomized controlled trials. Radiology 2002;224:47–54.
[9] Lo CM, Ngan H, Tso WK, et al. Randomized controlled trial of transarterial lipiodol chemoembolization for unresectable hepatocellular carcinoma. Hepatology 2002;35:1164–71.
[10] Llovet JM, Real MI, Montana X, et al. Arterial embolization or chemoembolization versus symptomatic treatment in patients with unresectable hepatocellular carcinoma: a randomized controlled trial. Lancet 2002;359:1734–9.
[11] Higuchi T, Kikuchi M, Okazaki M. Hepatocellular carcinoma after transcatheter hepatic arterial embolization. A histopathologic study of 84 resected cases. Cancer 1994;73:2259–67.
[12] Adachi E, Matsumata T, Nishizaki T, Hashimoto H, Tsuneyoshi M, Sugimachi K. Effects of preoperative transcatheter hepatic arterial chemoembolization for hepatocellular carcinoma. The relationship between postoperative course and tumor necrosis. Cancer 1993;72:3593–8.
[13] Phillips R, Murikami K. Preliminary neoplasms of the liver. Results of radiation therapy. Cancer 1960;13:714–20.
[14] Stillwagon GB, Order SE, Guse C, et al. 194 hepatocellular cancers treated by radiation and chemotherapy combinations: toxicity and response: a Radiation Therapy Oncology Group study. Int J Radiat Oncol Biol Phys 1989;17:1223–9.
[15] Zhao JD, Xu ZY, Zhu J, et al. Application of active breathing control in 3-dimensional conformal radiation therapy for hepatocellular carcinoma: the feasibility and benefit. Radiother Oncol 2008;87:439–44.
[16] Toya R, Murakami R, Baba Y, et al. Conformal radiation therapy for portal vein tumor thrombosis of hepatocellular carcinoma. Radiother Oncol 2007;84:266–71.
[17] Robertson JM, Lawrence TS, Dworzanin LM, et al. Treatment of primary hepatobiliary cancers with conformal radiation therapy and regional chemotherapy. J Clin Oncol 1993;11:1286–93.
[18] Suit HD, Goitein M, Munzenrider J, et al. Increased efficacy of radiation therapy by use of proton beam. Strahlenther Onkol 1990;166:40–4.
[19] Matsuzaki Y, Osuga T, Saito Y, et al. A new, effective, and safe therapeutic option using proton irradiation for hepatocellular carcinoma. Gastroenterology 1994;106:1032–41.
[20] Kanai T, Endo M, Minohara S, et al. Biophysical characteristics of HIMAC clinical irradiation system for heavy-ion radiation therapy. Int J Radiat Oncol Biol Phys 1999;44:201–10.
[21] Kanai T, Furusawa Y, Fukutsu K, Itsukaichi H, Eguchi-Kasai K, Ohara H. Irradiation of mixed beam and design of spread-out Bragg peak for heavy-ion radiotherapy. Radiat Res 1997;147:78–85.
[22] Kato H, Tsujii H, Miyamoto T, et al. Results of the first prospective study of carbon ion radiotherapy for hepatocellular carcinoma with liver cirrhosis. Int J Radiat Oncol Biol Phys 2004;59:1468–76.
[23] Kato H, Yamada S, Yasuda S, et al. Phase II study of short-course carbon ion radiotherapy (52.8GyE/4-fraction/1-week) for hepatocellular carcinoma. Hepatology 2005;42(Suppl. 1):381A.
[24] Blakely EA, Ngo FQH, Curtis SB, et al. Heavy ion radiobiology: cellular studies. Adv Radiat Biol 1984;11:295–378.
[25] Castro JR. Future research strategy for heavy ion radiotherapy. In: Kogelnih HD, editor. Progress in radio-oncology. Bologna: Monduzzi Editore; 1995. p. 643–8.
[26] Tsujii H, Morita S, Miyamoto T, et al. Preliminary results of phase I/II carbon ion therapy. J Brachyther Int 1997;13:1–8.
[27] Suzuki M, Kase Y, Yamaguchi H, Kanai T, Ando K. Relative biological effectiveness for cell-killing effect on various human cell lines irradiated with heavy-ion medical accelerator in Chiba (HIMAC) carbon-ion beams. Int J Radiat Oncol Biol Phys 2000;48:241–50.
[28] Hemming AW, Reed AI, Howard RJ, et al. Preoperative portal vein embolization for extended hepatectomy. Ann Surg 2003;237:686–91.
[29] Abulkhir A, Limongelli P, Healey AJ, et al. Preoperative portal vein embolization for major liver resection: a meta-analysis. Ann Surg 2008;247:49–57.
[30] Sato K, Yamada H, Ogawa K, et al. Performance of HIMAC. Nucl Phys 1995;A588:229–34.
[31] Minohara S, Kanai T, Endo M, Noda K, Kanazawa M. Respiratory gated irradiation system for heavy-ion radiotherapy. Int J Radiat Oncol Biol Phys 2000;47:1097–103.
[32] Kubo S, Shiomi S, Tanaka H, et al. Evaluation of the effect of portal vein embolization on liver function by (99m)tc-galactosyl human serum albumin scintigraphy. J Surg Res 2002;107:113–8.
[33] Kudo M, Todo A, Ikekubo K, Yamamoto K, Vera DR, Standalnik RC. Quantitative assessment of hepatocellular function through in vivo radioreceptor imaging with technetium 99m galactosyl human serum albumin. Hepatology 1993;17:814–9.
[34] Vera DR, Topcu SJ, Stadalnik RC. In vitro quantification of asialoglycoprotein receptor density from human hepatic microsamples. Methods Enzymol 1994;247:394–402.
[35] Reed Jr GB, Cox Jr AJ. The human liver after radiation injury. A form of veno-occlusive disease. Am J Pathol 1966;48:597–611.
[36] Lawrence TS, Robertson JM, Anscher MS, Jirtle RL, Ensminger WD, Fajardo LF. Hepatic toxicity resulting from cancer treatment. Int J Radiat Oncol Biol Phys 1995;31:1237–48.
[37] Cheng JC, Wu JK, Huang CM, et al. Radiation-induced liver disease after radiotherapy for hepatocellular carcinoma: clinical manifestation and dosimetric description. Radiother Oncol 2002;63:41–5.
[38] Heymsfield SB, Fulenwider T, Nordlinger B, Barlow R, Sones P, Kutner M. Accurate measurement of liver, kidney, and spleen volume and mass by computerized axial tomography. Ann Intern Med 1979;90:185–7.
[39] Moss AA, Friedman MA, Brito AC. Determination of liver, kidney, and spleen volumes by computed tomography: an experimental study in dogs. J Comput Assist Tomogr 1981;5:12–4.
[40] Sakamoto S, Uemoto S, Uryuhara K, et al. Graft size assessment and analysis of donors for living donor liver transplantation using right lobe. Transplantation 2001;71:1407–13.
[41] Zhou XP, Lu T, Wei YG, Chen XZ. Liver volume variation in patients with virus-induced cirrhosis: findings on MDCT. AJR Am J Roentgenol 2007;189:W153–159.
[42] Friedman LS, Martin P, Santiago JM. Liver function tests and the objective evaluation of the patient with liver disease. In: Zakim D, Boyer TD, editors. Hepatology. Philadelphia: WB Saunders; 1996. p. 791–833.
[43] Wants GE, Payne MA. Experience with portacaval shunt for portal hypertension. N Engl J Med 1961;265:721–8.
[44] Okuda K, Ohtsuki T, Obata H, et al. Natural history of hepatocellular carcinoma and prognosis in relation to treatment. Cancer 1985;56:918–28.
[45] Fong Y, Sun RL, Jarnagin W, et al. An analysis of 412 cases of hepatocellular carcinoma at a western center. Ann Surg 1999;229:790–9.
[46] Lee SP, Leu MY, Smathers JB, et al. Biologically effective dose distribution based on the linear quadratic model and its clinical relevance. Int J Radiat Oncol Biol Phys 1995;33:375–89.
[47] Karasu Z, Tekin F, Ersoz G, et al. Liver fibrosis is associated with decreased peripheral count in patients with chronic hepatitis B and C. Dig Dis Sci 2007;52:1535–9.

Jingu et al. Radiation Oncology 2010, 5:89
http://www.ro-journal.com/content/5/1/89

RADIATION ONCOLOGY

CASE REPORT Open Access

Carbon ion radiotherapy for basal cell adenocarcinoma of the head and neck: preliminary report of six cases and review of the literature

Keiichi Jingu*, Azusa Hasegawa, Jun-Etsu Mizo, Hiroki Bessho, Takamichi Morikawa, Hiroshi Tsuji, Hirohiko Tsujii, Tadashi Kamada

Abstract

Background: Basal cell adenocarcinoma accounts for approximately 1.6% of all salivary gland neoplasms. In this report, we describe our experiences of treatment for BCAC with carbon ion radiotherapy in our institution.

Methods: Case records of 6 patients with diagnosis of basal cell adenocarcinoma of the head and neck, who were treated by carbon ion radiotherapy with 64.0 GyE/16 fractions in our institution, were retrospectively reviewed.

Results: In a mean follow-up period of 32.1 months (14.0-51.3 months), overall survival and local control rates of 100% were achieved. Only one grade 4 (CTCAE v3.0) late complication occurred. There was no other grade 3 or higher toxicity.

Conclusions: Carbon ion radiotherapy should be considered as an appropriate curative approach for treatment of basal cell adenocarcinoma in certain cases, particularly in cases of unresectable disease and postoperative gross residual or recurrent disease.

Background

Basal cell adenocarcinoma (BCAC) was first recognized in 1978 and accounts for approximately 1.6% of all salivary gland neoplasms [1]. BCAC typically arises in adults older than 60 years of age and has no gender predominance [2]. The vast majority of BCACs occur in the parotid gland (about 90%) [3-5], followed by the submandibular gland and minor salivary glands [6]. The 2005 WHO classification categorizes BCAC as a low-grade tumor with a favorable prognosis [7]. The standard treatment has been wide local excision with or without postoperative radiotherapy. However, local recurrence has frequently been reported.

Carbon ion radiation therapy (C-ion RT) was initiated at the National Institute of Radiological Sciences (NIRS) in 1994 [8]. For malignant tumors of the head and neck, a phase II clinical trial with C-ion RT was started in April 1997. So far, we have treated more than 350 patients with a large histological variety of malignant tumors of the head and neck including mainly mucosal malignant melanoma and adenoid cystic carcinoma. Of those patients, 6 patients with BCAC of the head and neck were enrolled. In this report, we describe the 6 patients with BCAC and the efficacy and complications of C-ion RT.

Methods

Case Presentation

The 6 patients' characteristics are shown in Table 1. Mean age was 58 years (range: 37-81 years). None of the patients had metastasis in distant organs. The primary sites were parotid gland in 4 patients, base of the tongue in 1 patient and ethmoid sinus in 1 patient. The stages for all patients were defined according to Unio Internationalis Contra Cancrum (UICC) 2002. Histology of all patients was reconfirmed by a pathologist in our institution before C-ion RT.

* Correspondence: kjingu@nirs.go.jp
Research Center for Charged Particle Therapy, National Institute of Radiological Sciences (NIRS), Chiba, Japan

Table 1 Patients' Characteristics

Patient	Age	Gender	Primary Site	Stage (UICC§ 2002)	Tumor Response (RECIST*)	Grade 3 or more Toxicities (CTCAE† v3.0)	Observation Period (months)
1	43	M	base of tongue	cT4aN0M0	PR	none	25.9
2	70	M	ethmoid sinus	cT4aN0M0	PR	Grade 4 retinopathy	20.9
3	62	F	parotid grand	postoperative recurrence (pT3N0M0, R0)	CR	none	14.0
4	37	F	parotid grand	cT3N1M0	PR	none	49.6
5	81	M	parotid grand	cT4aN0M0	SD	none	51.3
6	55	M	parotid grand	postoperative residual (pT4aN0M0, R2)	CR	none	31.3

Abbreviation, §Unio Internationalis Contra Cancrum; *Response Evaluation Criteria in Solid Tumors; †Common Terminology Criteria for Adverse Events.

Clinical Histories

Patient 1

A 43-year-old Japanese male developed a sore throat over a period of 3 months. A tumor at the base of the tongue was detected by endoscopy. The pathological diagnosis was BCAC by biopsy. CT revealed that the clinical stage was T4aN0M0 (stage IVA). The diameter of the primary tumor was 29 mm. At first, one cycle of chemotherapy, including cisplatin, 5-FU and docetaxel, was performed in the previous hospital; however, the tumor did not show shrinkage. He therefore came to our institution for C-ion RT.

Patient 2

A 70-year-old Japanese male had nasal bleeding for one week. A tumor in the right ethmoid sinus was detected by endoscopy and CT in the previous hospital. Biopsy was performed in the previous hospital, and the diagnosis was BCAC (MIB-1 index, 50-80%) in the right ethmoid sinus with intracranial invasion. The diameter of the primary tumor was 50 mm and there was no lymphadenopathy (cT4aN0M0, stage IVA). There was no indication for surgery. He came to our institution for C-ion RT. The patient had bilateral retinal detachments as a past history.

Patient 3

A 62-year-old Japanese female had undergone right total parotidectomy in the previous hospital (pT3N0M0, stage III, R0). The pathological diagnosis was BCAC. Thereafter, follow-up was performed every 3 months. Eight years after parotidectomy, a tumor of 54 mm in diameter was detected under the right temporal skin by MRI, and BCAC recurrence was confirmed by biopsy. No lymphadenopathy was detected. There was no indication for surgery. She came to our institution for C-ion RT.

Patient 4

A 37-year-old Japanese female developed fullness in the right ear and right buccal swelling over a period of 3 months. She underwent fine needle biopsy and was diagnosed as cytologic class III in the previous hospital. Total parotidectomy +/- postoperative radiotherapy was planned. CT revealed that the clinical stage was T3N1M0 (stage III). The diameter of the primary tumor was 54 mm and the diameter of the right upper cervical lymph node was 18 mm. However, she declined surgery and requested C-ion RT. We required the previous hospital to perform biopsy for confirming the histology. Thereafter, her tumor was diagnosed as BCAC (MIB-1 index, 10%).

Patient 5

An 81-year-old Japanese male developed left buccal swelling over a period of one and half years. A benign tumor was suspected by CT, but the histological diagnosis was BCAC by biopsy. The clinical stage was T4aN0M0 (stage IVA). The diameter of the primary tumor was 52 mm and there was no lymphadenopathy. If curative surgery was performed, facial nerve palsy could not be avoided. For this reason, he declined curative surgery and selected C-ion RT.

Patient 6

A 55-year-old Japanese male had right buccal swelling. A benign tumor was suspected and observation was performed. Four years later, a gastric malignant tumor was found by medical examination. Right partial parotidectomy was performed simultaneously with total gastric resection. The histological diagnosis of the parotid tumor was BCAC with suspected residual macroscopic tumor (pT4aN0M0, stage IVA, R2). For gastric cancer, chemotherapy including TS-1 was performed for 6 months after surgery. However, a gross tumor of 19 mm in diameter in his right parotid gland remained. He selected C-ion RT.

Treatment

All of the patients were not indicated for curative surgery or declined surgery, and C-ion RT was performed as follows.